Copy 1
RM SL56C26

Declassified. 6/18/69
NASA. TD #172.

Declassified by authority of NASA
Classification Change Notices No. 132
Dated ** 8/30/69

NACA

ORIGINAL REPORT

RESEARCH MEMORANDUM

for the

Bureau of Aeronautics, Department of the Navy

PRELIMINARY INVESTIGATION OF THE STATIC

LONGITUDINAL AND LATERAL STABILITY CHARACTERISTICS

OF A 1/20-SCALE MODEL OF THE McDONNELL F4H-1 AIRPLANE

AT MACH NUMBERS OF 1.59, 1.89, and 2.09

TED NO. NACA AD 3115

By Melvin M. Carmel and Donald T. Gregory

Langley Aeronautical Laboratory
Langley Field, Va.

SERVICE REPORT

NATIONAL ADVISORY COMMITTEE
FOR AERONAUTICS
WASHINGTON

MAR 23 1956

DECLASSIFIED

CONFIDENTIAL

NATIONAL ADVISORY COMMITTEE FOR AERONAUTICS

RESEARCH MEMORANDUM

Declassified by authority of NASA Classification Change Notices No. 122

for the

*Dated ** 8/30/69*

Bureau of Aeronautics, Department of the Navy

PRELIMINARY INVESTIGATION OF THE STATIC

LONGITUDINAL AND LATERAL STABILITY CHARACTERISTICS

OF A 1/20-SCALE MODEL OF THE McDONNELL F4H-1 AIRPLANE

AT MACH NUMBERS OF 1.59, 1.89, and 2.09

TED NO. NACA AD 3115

By Melvin M. Carmel and Donald T. Gregory

SUMMARY

An abbreviated investigation was performed in the Langley Unitary Plan wind tunnel to determine the drag, longitudinal stability, and lateral stability characteristics of a 1/20-scale model of the McDonnell F4H-1 airplane. The tests were made at Mach numbers of 1.59, 1.89, and 2.09 at Reynolds numbers of 1.9×10^6, 1.8×10^6, and 1.7×10^6, respectively. The Reynolds numbers are based on the mean aerodynamic chord of the wing.

INTRODUCTION

At the request of the Bureau of Aeronautics, Department of the Navy, an investigation of the aerodynamic characteristics of a 1/20-scale model of the McDonnell F4H-1 airplane at supersonic speeds has been undertaken by the National Advisory Committee for Aeronautics.

Inasmuch as tunnel time for an extensive test program was unavailable, an interim program has been undertaken to satisfy the urgent need for a brief evaluation of the drag and directional stability characteristics of the airplane.

CONFIDENTIAL

The present paper contains results obtained at Mach numbers of 1.59, 1.89, and 2.09 in the Langley Unitary Plan wind tunnel.

COEFFICIENTS AND SYMBOLS

b wing span, in.

$\bar{c}$ mean aerodynamic chord, in.

$\bar{c}_t$ mean aerodynamic chord of horizontal tail, in.

$C_D{}'$ drag coefficient, D/qS

C_{D_B} base drag coefficient, $\dfrac{D_{base}}{qS}$

C_{D_i} internal duct drag coefficient, $\dfrac{D_{internal}}{qS}$

C_L lift coefficient, L/qS

C_m pitching-moment coefficient, $m/qS\bar{c}$

C_l rolling-moment coefficient, l/qSb

C_n yawing-moment coefficient, n/qSb

C_Y lateral force, Y/qS

C_{h_t} horizontal-tail hinge-moment coefficient, $h_t/q\bar{c}_t S_H$

C_{N_t} normal-force coefficient of horizontal tail, N_t/qS_H

D drag, lb

L lift, lb

m pitching moment, in-lb

l rolling moment, in-lb

n yawing moment, in-lb

Y	lateral force, lb
h_t	horizontal-tail hinge moment, in-lb
N_t	normal force on horizontal tail, lb
M	free-stream Mach number
p	free-stream static pressure, lb/sq ft
q	free-stream dynamic pressure, $0.7pM^2$, lb/sq ft
S	wing area including body intercept, sq ft
S_H	horizontal-tail area (theoretical), sq ft
i_t	stabilator angle, deg from water line
α	angle of attack of wing, deg
β	angle of sideslip of fuselage center line, deg
F.S.	fuselage station
B.L.	body line
W.L.	water line

The results of these tests are presented as standard NACA coefficients of forces and moments referred to the stability-axes system. All aerodynamic moments were taken about the center of gravity of the model, which is longitudinally located at $0.30\bar{c}$, and at a station 0.976 inch above the root chord. The hinge moments for the horizontal tail were taken about $0.41\bar{c}_t$.

APPARATUS AND METHODS

Tunnel

The tests were conducted in the low Mach number test section of the Langley Unitary Plan wind tunnel. This tunnel is a variable-pressure, continuous, return-flow type. The test section is 4 feet square and approximately 7 feet in length. The nozzle leading to the test section

is of the asymmetric sliding-block type and variable Mach number may be obtained continuously through a Mach number range from approximately 1.59 to 2.7 without tunnel shutdown.

Model and Support System

The 1/20-scale steel model was constructed by McDonnell Aircraft Company. A three-view drawing of the model is presented as figure 1. Photographs of the test model are presented in figure 2. Details of the Sparrow stores installation on the model are presented in figure 3. The geometric characteristics of the model are presented in table I.

The model was attached to the forward end of an enclosed six-component electrical strain-gage balance. This balance was attached, by means of a sting, to the central support system of the tunnel.

Additional components of the support system for the model consisted of a rotary sting, an adapter to fit the model sting, and a 10° bent coupling. The rotary sting is one which will rotate $\pm 90^O$ about the longitudinal axis of the sting support. The sting support will move approximately $\pm 15^O$ in the horizontal plane. The rotary sting is between the bent coupling and the sting support. This is a feature used by the Unitary Plan wind tunnel at the present time for obtaining combination angles of attack and sideslip for models. The bent coupling was necessary in order to obtain the desired range of angle of attack for the current tests.

The model was instrumented with a strain-gage balance on the horizontal tail for the purpose of obtaining horizontal-tail normal force and hinge moments.

Measurements and Accuracy

Tests were made through an angle-of-attack range of -2^O to 19° for a sideslip angle of 0°. At angles of attack of 0° and 15°, the sideslip-angle range was from -4° to 9°; at an angle of 8°, the sideslip-angle range extended to 12°. The model was tested at each attitude at all three Mach numbers. All angles of attack and angles of sideslip were corrected for the deflection of the balance and the sting under load conditions. These angles are estimated to be accurate within $\pm 0.1^O$. The maximum deviation of local Mach number in the portion of the tunnel occupied by the model was ± 0.015 from the average values given.

The dewpoint temperature for all tests was maintained below -30°. The stagnation temperature was approximately 120° F and the stagnation pressure was maintained at approximately 9 lb/sq in. abs.

The accuracy of the force and moment coefficients, based on balance calibration and reproducibility of the data, is estimated to be within the following limits:

C_L . . . . ± 0.002

C_D' . . . . ± 0.001

C_m . . . . ± 0.001

C_l . . . . ± 0.0002

C_n . . . . ± 0.0005

C_Y . . . . ± 0.0015

C_{h_t} . . . . ± 0.002

C_{N_t} . . . . ± 0.002

The tunnel, as yet, has not been completely calibrated, and any flow angularity that might exist in the tunnel has not been determined. The lift-coefficient data presented in this report for sideslip tests are asymmetrical about the tunnel center line and there is the possibility that this phenomenon may be the result of flow angularity. Tunnel pressure gradients in the region of the model have been determined and are sufficiently small so as not to induce any buoyancy effect on the model.

and therefore C_D & C_m

The drag data have been adjusted so that the balance-chamber pressures represent free-stream static pressure. The base drag coefficients for the model with stores are presented in figure 4 in order to show the relative magnitudes of these coefficients for this model. In order to obtain as accurate a base drag coefficient as possible, pressures were taken, not only near the balance, but also on the upper and lower surfaces of the gooseneck sting in the vicinity of the model where such pressures would be felt by the model in an axial direction. These pressures, when acting in a lift direction, add only an insignificant increment to the lift and pitching moment of the model.

The internal-duct drag of the model was obtained for pitch runs only for angles of attack from -2° to 9°. This drag was obtained by two methods. The first method consisted of a 22-tube rake at the duct exit with a multihole choker placed about 2 diameters forward of the end of the rake tubes. The second method of obtaining internal-duct drag consisted of placing a single total-pressure tube 1/8 of an inch forward of a single-hole choker which had the same opening area as that for the multihole choker. The rakes for each type of pressure measurement were mounted completely free of the model.

The data obtained with the multihole choker showed supersonic flow at the measuring-rake station. It is believed that the rake was too close to the choker and in a region in which the air flow had not reached equilibrium. Accordingly, these data are not presented in this report.

The internal-duct-drag data obtained with the single total-pressure tube is believed to be a true representation of this drag for the model. The internal drag is measured only from the entrance of the duct to the choke station in the model, and thus a small amount of pressure drag still exists between the choke and the end of the model duct. The measured internal drag coefficients, plotted against angle of attack for the three test Mach numbers, are presented in figure 5. To obtain the net external drag, these coefficients must be subtracted from those obtained by strain-gage measurements.

The inlet mass-flow ratios at Mach numbers of 1.59, 1.89, and 2.09 for $\alpha = \beta = 0^{\circ}$ were 0.93, 0.96, and 0.97, respectively.

A study of the force results in conjunction with the schlieren photographs available (fig. 6) indicates little or no shock reflection effect on the model for any of the test configurations or attitudes at Mach numbers of 1.89 and 2.09. There is the possibility that for a Mach number of 1.59 there are small shock reflection effects on the model, especially at the higher angles of sideslip, for all angles of attack. The aft end of the model was altered considerably from the true shape of the airplane in order to house the sting support. (See fig. 2.) Before the tests were begun, it was known that this type of model support would affect the stability results of the investigation. For the sake of expedience, however, it was decided to perform the tests in order to get a preliminary idea of the stability characteristics of the airplane and to determine stability trends at the high Mach number range of the tests. There was, as expected, an effect of the sting on the horizontal tail, resulting from shock waves emanating from the sting and from the effect of the sting on the pressure distribution around the tail, at all test Mach numbers and model attitudes. The effect of the sting would be felt primarily on pitching moment, tail normal force, and horizontal-tail hinge moment, and consequently exact numbers for these aerodynamic characteristics were impossible to obtain. For comparative purposes, the lift-curve slope of the horizontal tail was computed theoretically and found to be about twice as great as the experimental lift-curve slope at all test Mach numbers. This serves as some indication of the effect of the sting on the horizontal tail.

PRESENTATION OF RESULTS

The results of the investigation are presented in the following figures:

RESULTS

The basic results are presented without analysis; however, some
general observations relative to the data are as follows:

1. The minimum drag coefficients for the complete model with a tail
incidence of 0° are 0.038, 0.034, and 0.033 at Mach numbers of 1.59, 1.89,
and 2.09, respectively. These values of drag coefficient are with the
internal-duct drag subtracted to give net external drag coefficient. It
must be remembered that trim drag coefficients for the airplane will
necessarily be somewhat higher than these values.

2. The neutral point for all configurations of the complete model
is located at approximately 61.5 percent of the mean aerodynamic chord
for all test Mach numbers. For the model without the horizontal tail
the neutral point is located at approximately 48 percent of the mean
aerodynamic chord.

3. The horizontal-tail-incidence range tested did not encompass
trim conditions for this airplane flying at the test Mach numbers.
Extrapolation of the data for the airplane with combat loading at an
altitude of 50,000 feet indicates that (a) for a Mach number of 1.59,
the lift coefficient for trim will be about 0.151 with $i_t = -9.2^{\circ}$;

(b) $M = 1.89$ and $C_{L_{trim}} = 0.107$ with $i_t = -9^{\circ}$; (c) $M = 2.09$ and

$C_{L_{trim}} = 0.087$ with $i_t = -9.2^{\circ}$.

4. The results indicate positive static directional stability for
complete model configurations at angles of attack to 15° in the test Mach
number range. The directional stability, however, decreased somewhat with
Mach number and is relatively unaffected by increase in angle of attack
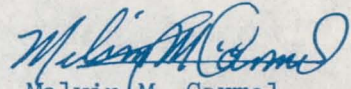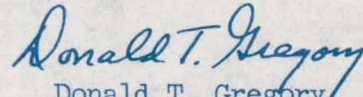for the range between 0° and 15°.

8

5. The data indicate negative effective dihedral at angles of attack of 0.3° and 8.5° for model configurations with and without the vertical tail. At an angle of attack of 15.7°; positive effective dihedral is indicated for these two conditions.
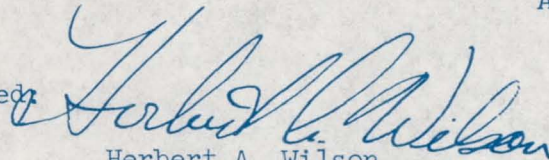
Langley Aeronautical Laboratory,
    National Advisory Committee for Aeronautics,
        Langley Field, Va., March 2, 1955.

Melvin M. Carmel
Aeronautical Research Scientist

Donald T. Gregory
Aeronautical Research Scientist

Approved:

Herbert A. Wilson
Chief of Unitary Wind Tunnel

pwm

DECLASSIFIED CONFIDENTIAL

TABLE I.— GEOMETRIC CHARACTERISTICS OF THE F4H-1 MODEL

[Fuselage station 0.00 is 8.4 inches aft of nose (full scale)]

```
Model scale, percent . . . . . . . . . . . . . . . . . . . . . . . . . . . . . . . . . . . . . . . .    5
Center-of-gravity location, percent of mean aerodynamic chord . . . . . . . . . . . . . . . . .   30
Wing:
    Loading (combat), lb/sq ft . . .  . . . . . . . . . . . . . . . . . . . . . . . . . . . . .   65
    Area, sq ft:
        Exposed . . . . . . . . . . . . . . . . . . . . . . . . . . . . . . . . . . . . . . . .  0.886
        Theoretical . . . . . . . . . . . . . . . . . . . . . . . . . . . . . . . . . . . . . .  1.325
    Span, in. . . . . . . . . . . . . . . . . . . . . . . . . . . . . . . . . . . . . . . . . .  23.2
    Aspect ratio . . . . . . . . . . . . . . . . . . . . . . . . . . . . . . . . . . . . . . . .  2.821
    Taper ratio . . . . . . . . . . . . . . . . . . . . . . . . . . . . . . . . . . . . . . . .  0.167
    Sweep angle of quarter-chord line, deg . . . . . . . . . . . . . . . . . . . . . . . . . . .   45
    Dihedral, deg . . . . . . . . . . . . . . . . . . . . . . . . . . . . . . . . . . . . . . .    0
    Incidence, deg . . . . . . . . . . . . . . . . . . . . . . . . . . . . . . . . . . . . . . .    1
    Geometric twist, deg . . . . . . . . . . . . . . . . . . . . . . . . . . . . . . . . . . . .    0
    Airfoil:
        Root . . . . . . . . . . . . . . . . . . . . . . . . . . . . . . . NACA 0006.4-64 (modified)
        B.L. 160 (full scale) . . . . . . . . . . . . . . . . . . . . . . . NACA 0004-64 (modified)
        Tip . . . . . . . . . . . . . . . . . . . . . . . . . . . . . . . . NACA 0003-64 (modified)
    Root chord, in. . . . . . . . . . . . . . . . . . . . . . . . . . . . . . . . . . . . . . .  14.10
    Tip chord, in. . . . . . . . . . . . . . . . . . . . . . . . . . . . . . . . . . . . . . . .  2.35
    Root-chord location:
        Longitudinal (leading edge) . . . . . . . . . . . . . . . . . . . . . . . . . . . F.S. 7.518
        Vertical . . . . . . . . . . . . . . . . . . . . . . . . . . . . . . . . . . . . . W.L. 0.574
    Mean aerodynamic chord, in. . . . . . . . . . . . . . . . . . . . . . . . . . . . . . . . .  9.63
    Mean-aerodynamic-chord location:
        Longitudinal (leading edge) . . . . . . . . . . . . . . . . . . . . . . . . . . . F.S. 13.054
        Lateral . . . . . . . . . . . . . . . . . . . . . . . . . . . . . . . . . . . . . . B.L. 4.42
Fuselage:
    Length, in. . . . . . . . . . . . . . . . . . . . . . . . . . . . . . . . . . . . . . . . .  33.60
    Width (maximum), in.  . . . . . . . . . . . . . . . . . . . . . . . . . . . . . . . . . . .  3.375
    Depth (maximum), in.  . . . . . . . . . . . . . . . . . . . . . . . . . . . . . . . . . . .  3.730
    Overall fineness ratio . . . . . . . . . . . . . . . . . . . . . . . . . . . . . . . . . . .  8.40
    Base area . . . . . . . . . . . . . . . . . . . . . . . . . . . . . . . . . . . . . . . . .  None
Horizontal tail:
    Area (theoretical), sq ft . . . . . . . . . . . . . . . . . . . . . . . . . . . . . . . . .  0.237
    Span, in. . . . . . . . . . . . . . . . . . . . . . . . . . . . . . . . . . . . . . . . . .  10.626
    Aspect ratio . . . . . . . . . . . . . . . . . . . . . . . . . . . . . . . . . . . . . . . .  3.31
    Taper ratio . . . . . . . . . . . . . . . . . . . . . . . . . . . . . . . . . . . . . . . .  0.200
    Root chord, in. . . . . . . . . . . . . . . . . . . . . . . . . . . . . . . . . . . . . . .  5.35
    Tip chord, in. . . . . . . . . . . . . . . . . . . . . . . . . . . . . . . . . . . . . . . .  1.07
    Mean aerodynamic chord, in. . . . . . . . . . . . . . . . . . . . . . . . . . . . . . . . .  3.686
    Mean-aerodynamic-chord location:
        Longitudinal (leading edge) . . . . . . . . . . . . . . . . . . . . . . . . . . . . F.S. 29.16
        Lateral . . . . . . . . . . . . . . . . . . . . . . . . . . . . . . . . . . . . . . B.L. 2.066
    Tail length (distance from quarter-chord point of mean
        aerodynamic chord of wing to quarter-chord point of
        mean aerodynamic chord of horizontal tail), in. . . . . . . . . . . . . . . . . . . . .  14.619
    Sweep angle of quarter-chord line, deg . . . . . . . . . . . . . . . . . . . . . . . . . . .  35.5
    Dihedral, deg . . . . . . . . . . . . . . . . . . . . . . . . . . . . . . . . . . . . . . .   -15
    Geometric twist, deg . . . . . . . . . . . . . . . . . . . . . . . . . . . . . . . . . . . .    0
    Airfoil:
        Root . . . . . . . . . . . . . . . . . . . . . . . . . . . . . . . . NACA 0003.7-64 (modified)
        Tip . . . . . . . . . . . . . . . . . . . . . . . . . . . . . . . . . NACA 0003-64 (modified)
Vertical tail (including rudder)
    Area (theoretical), sq ft . . . . . . . . . . . . . . . . . . . . . . . . . . . . . . . . .  0.1751
    Span, in. . . . . . . . . . . . . . . . . . . . . . . . . . . . . . . . . . . . . . . . . .  3.825
    Aspect ratio . . . . . . . . . . . . . . . . . . . . . . . . . . . . . . . . . . . . . . . .  0.5802
    Taper ratio . . . . . . . . . . . . . . . . . . . . . . . . . . . . . . . . . . . . . . . .  0.2691
    Root chord, in. . . . . . . . . . . . . . . . . . . . . . . . . . . . . . . . . . . . . . .  8.750
    Tip chord, in. . . . . . . . . . . . . . . . . . . . . . . . . . . . . . . . . . . . . . . .  2.355
    Mean aerodynamic chord, in. . . . . . . . . . . . . . . . . . . . . . . . . . . . . . . . .  6.166
    Mean-aerodynamic-chord location:
        Longitudinal (leading edge) . . . . . . . . . . . . . . . . . . . . . . . . . . . F.S. 25.955
        Vertical (leading edge) . . . . . . . . . . . . . . . . . . . . . . . . . . . . . . W.L. 4.87
    Tail length (distance from quarter-chord point of mean
        aerodynamic chord of wing to quarter-chord point of
        mean aerodynamic chord of vertical tail), in. . . . . . . . . . . . . . . . . . . . . .  12.028
    Airfoil:
        Root . . . . . . . . . . . . . . . . . . . . . . . . . . . . . . . . NACA 0003.2-64 (modified)
        Tip . . . . . . . . . . . . . . . . . . . . . . . . . . . . . . . . . NACA 0002.5-64 (modified)
Duct:
    Inlet area, sq ft per side . . . . . . . . . . . . . . . . . . . . . . . . . . . . . . . . .  0.00855
    Compressor face, sq ft per side . . . . . . . . . . . . . . . . . . . . . . . . . . . . . .  0.0131
    Exit, sq ft per side . . . . . . . . . . . . . . . . . . . . . . . . . . . . . . . . . . . .  0.0169
```

Figure 1.- Three-view drawing of 1/20-scale model of the McDonnell F4H-1 airplane. All dimensions are in inches unless otherwise specified.
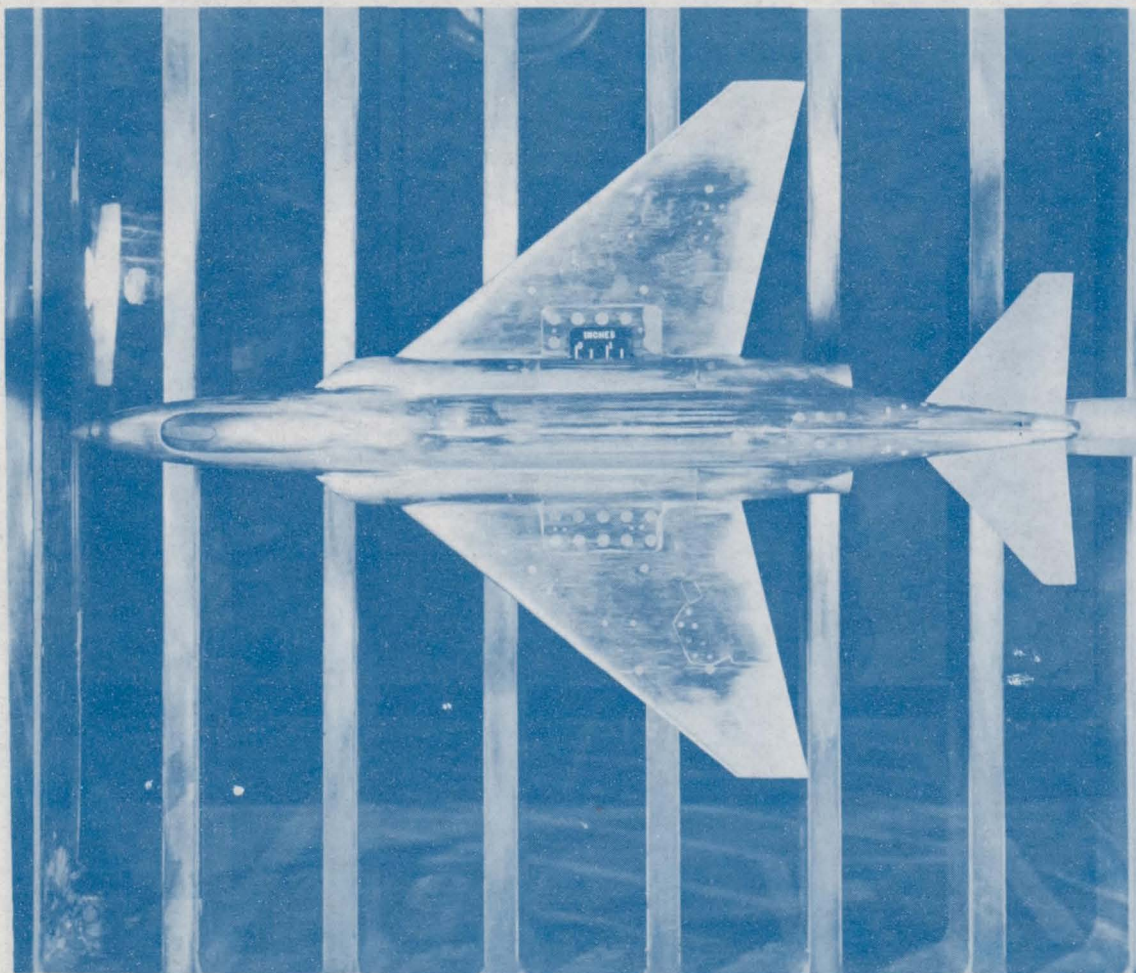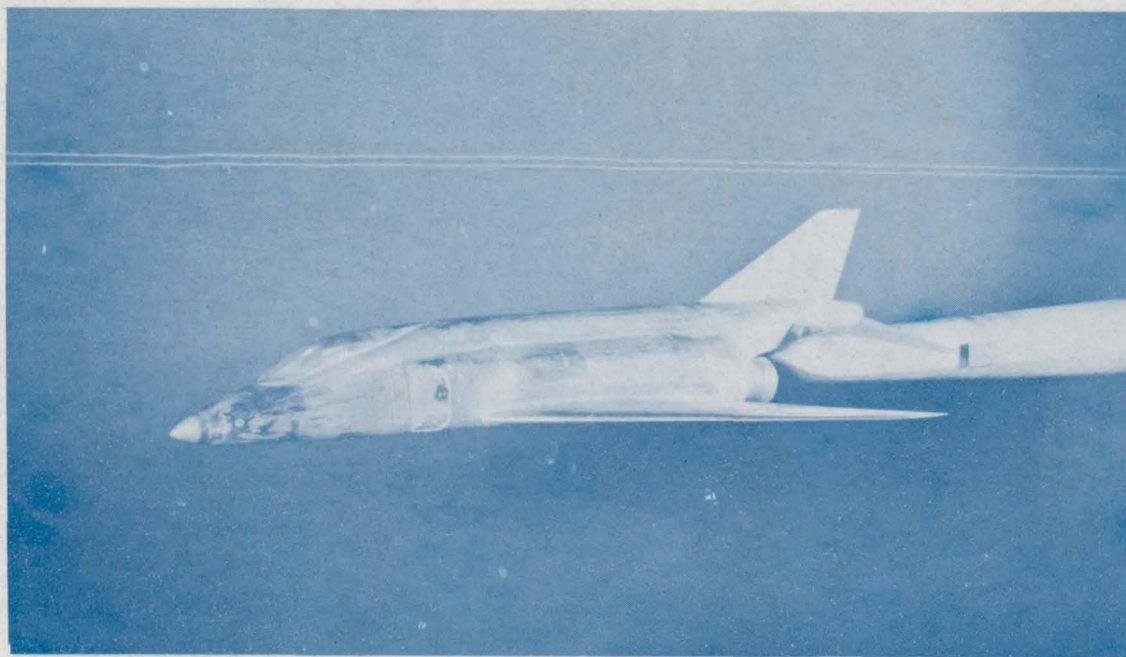
(a) Top view.   L-91477

Figure 2.- Photographs of 1/20-scale model of the McDonnell F4H-1 airplane.
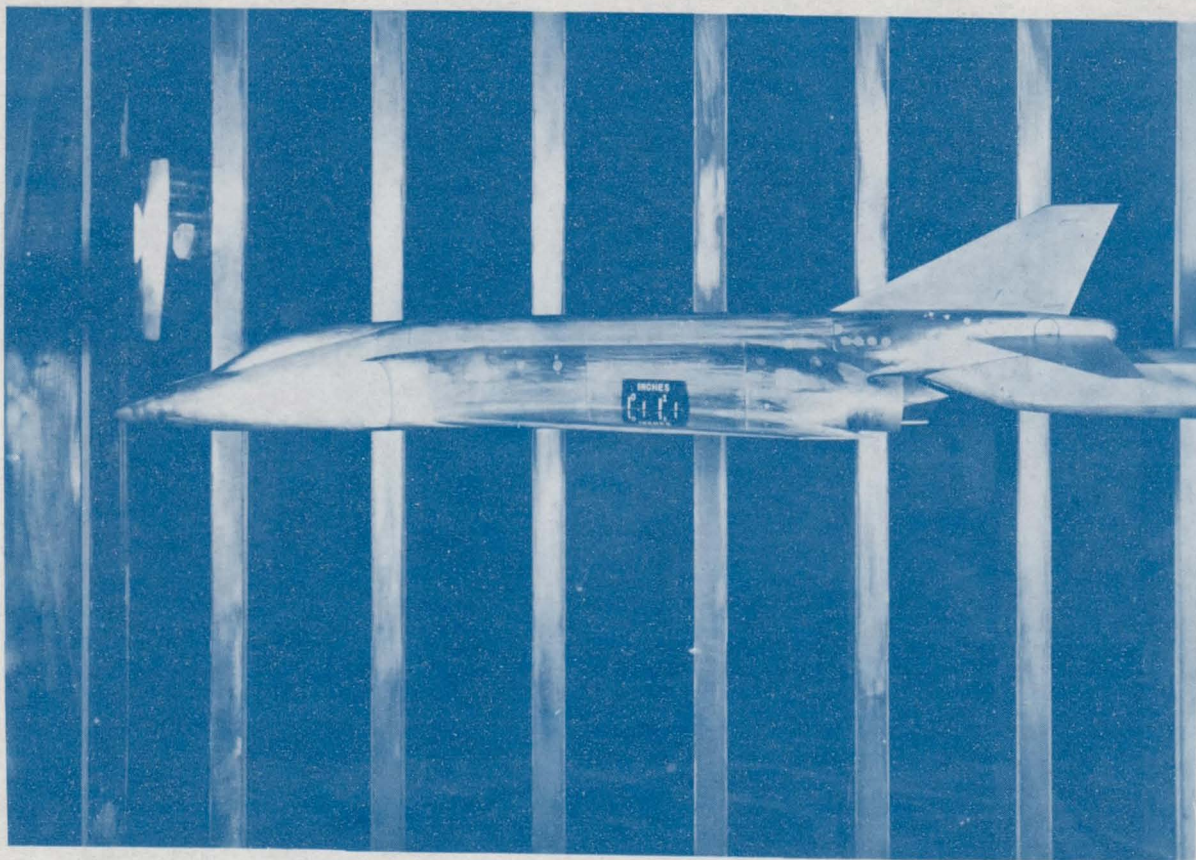
(b) Three-quarter front view.

L-91478

Figure 2.- Continued.

(c) Side view.

L-91479

Figure 2.- Continued.
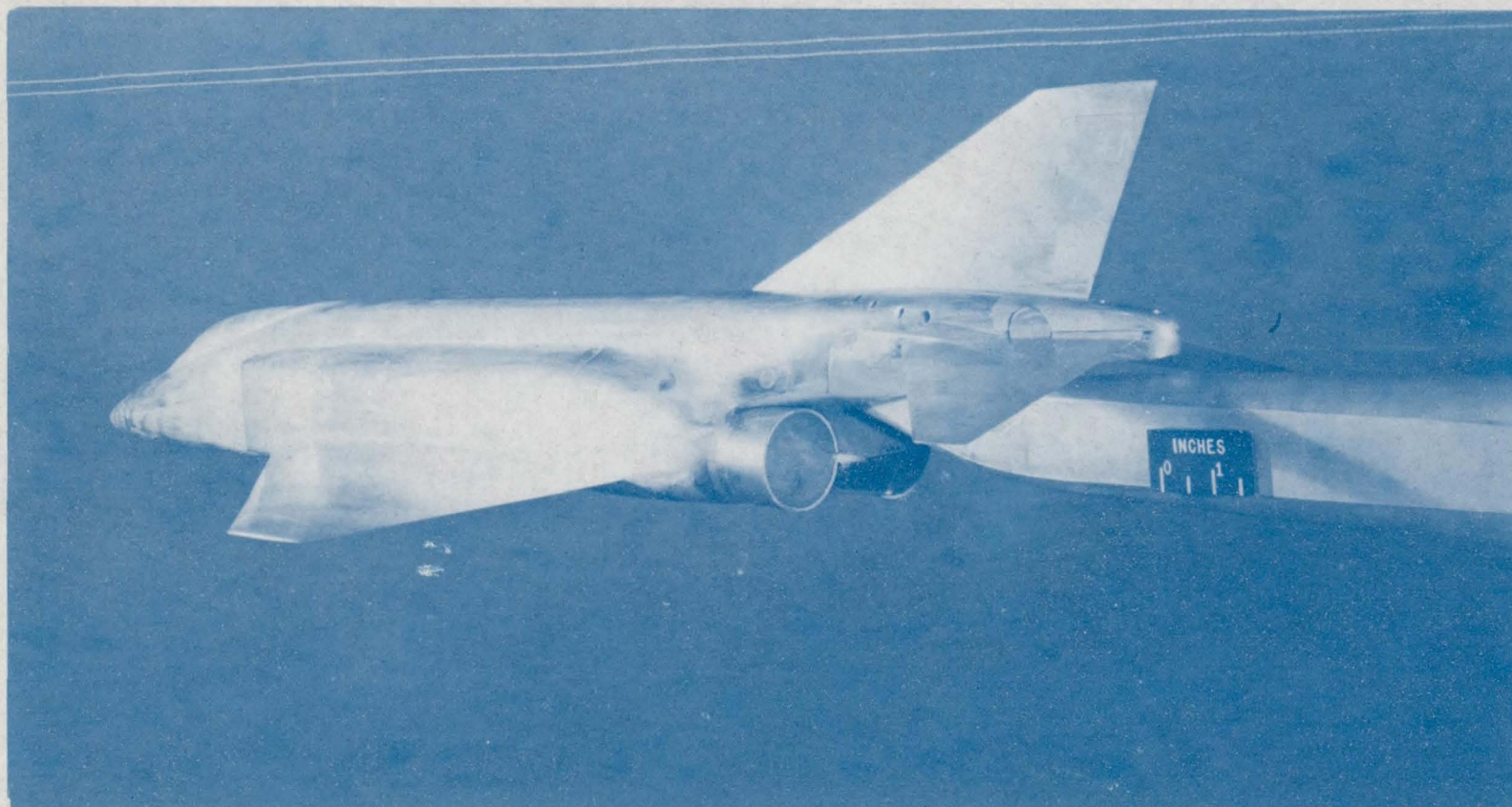
(d) Three-quarter rear view.

L-91480

Figure 2.- Concluded.

DECLASSIFIED

F.S. 5.25
W.L. 0.143
B.L. 0.86

Missile ₵

F.S. 12.40
W.L. 0.062
B.L. 1.143

W.L. 0.00

C

C

Section A-A

F.S. 15.98
W.L. 0.06
B.L. 2.245

Missile ₵

F.S. 23.13
W.L. -0.148
B.L. 2.245

W.L. 0.0

D

D

Section B-B

W.L. 0.00

2° 30'

3° 15'

Section C-C

Section D-D
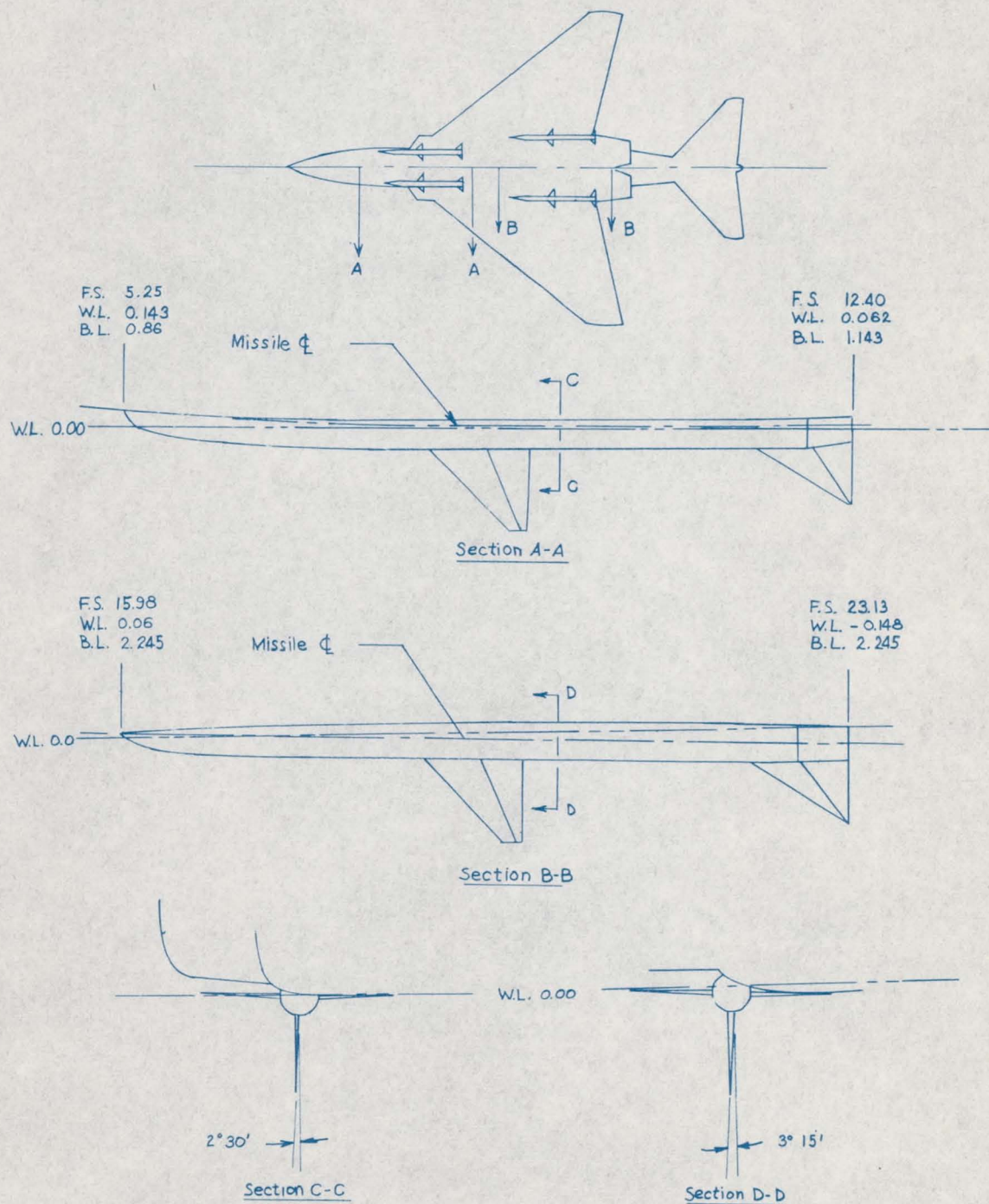
Figure 3.- Sparrow stores installation on 1/20-scale model of the
McDonnell F4H-1 airplane.

DE CLASSIFIED
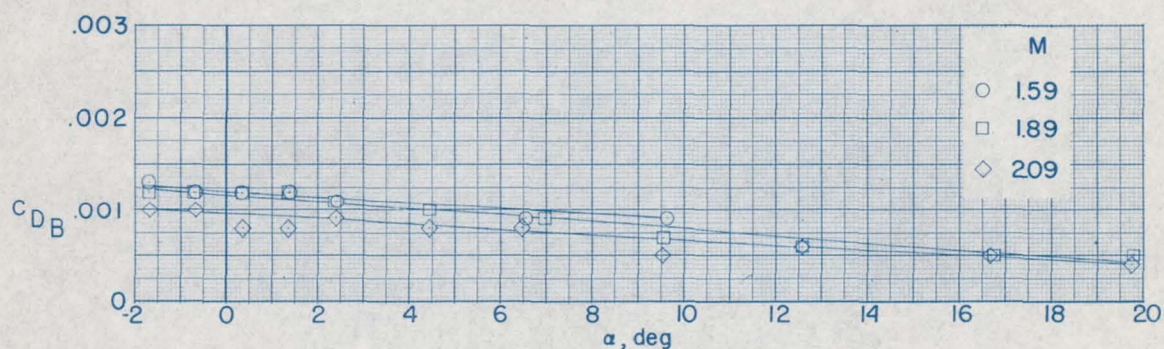
Figure 4.- Variation of base drag coefficient with angle of attack for
the 1/20-scale model of the McDonnell F4H-1 airplane with external
stores.
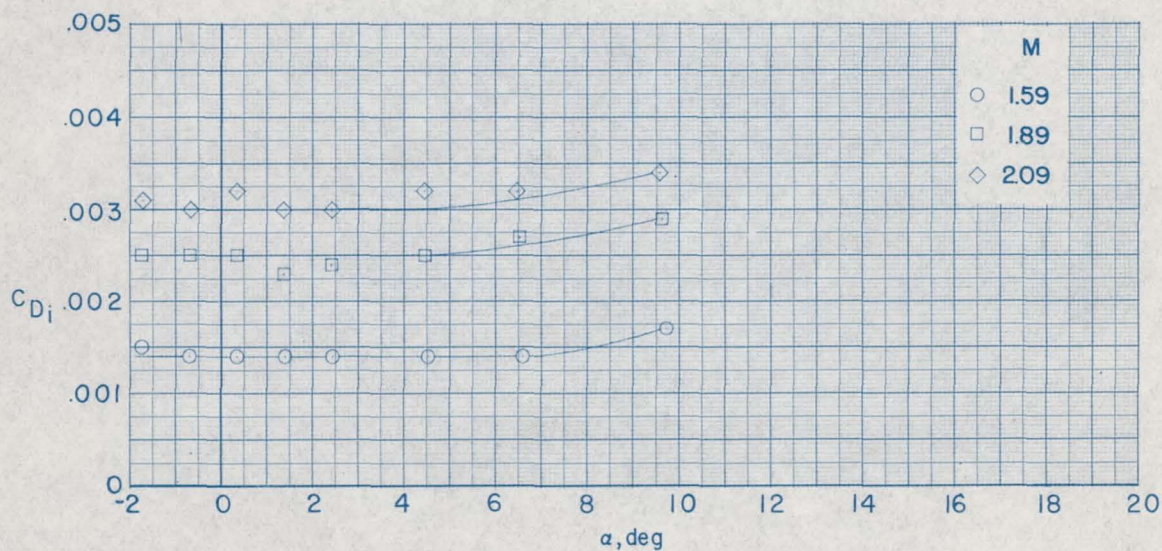
Figure 5.- Variation of internal-duct drag coefficient with angle of
attack for the 1/20-scale model of the McDonnell F4H-1 airplane
without horizontal tail.

M=1.89
α =19.9 deg
β =0 deg

M=2.09
α =19.9 deg
β =0 deg

M=1.59
α =8.5 deg
β =10.5 deg
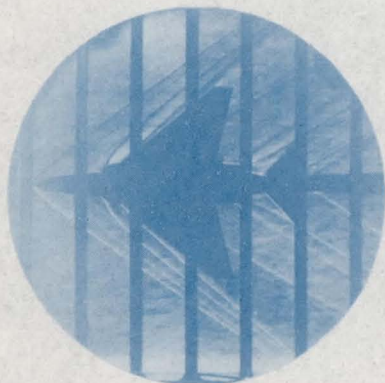
M=1.89
α =1.4 deg
β =0 deg

M=2.09
α =0.3 deg
β =0 deg

L-92446

Figure 6.- Typical schlieren photographs of 1/20-scale model of
McDonnell F4H-1 airplane.

DECLASSIFIED
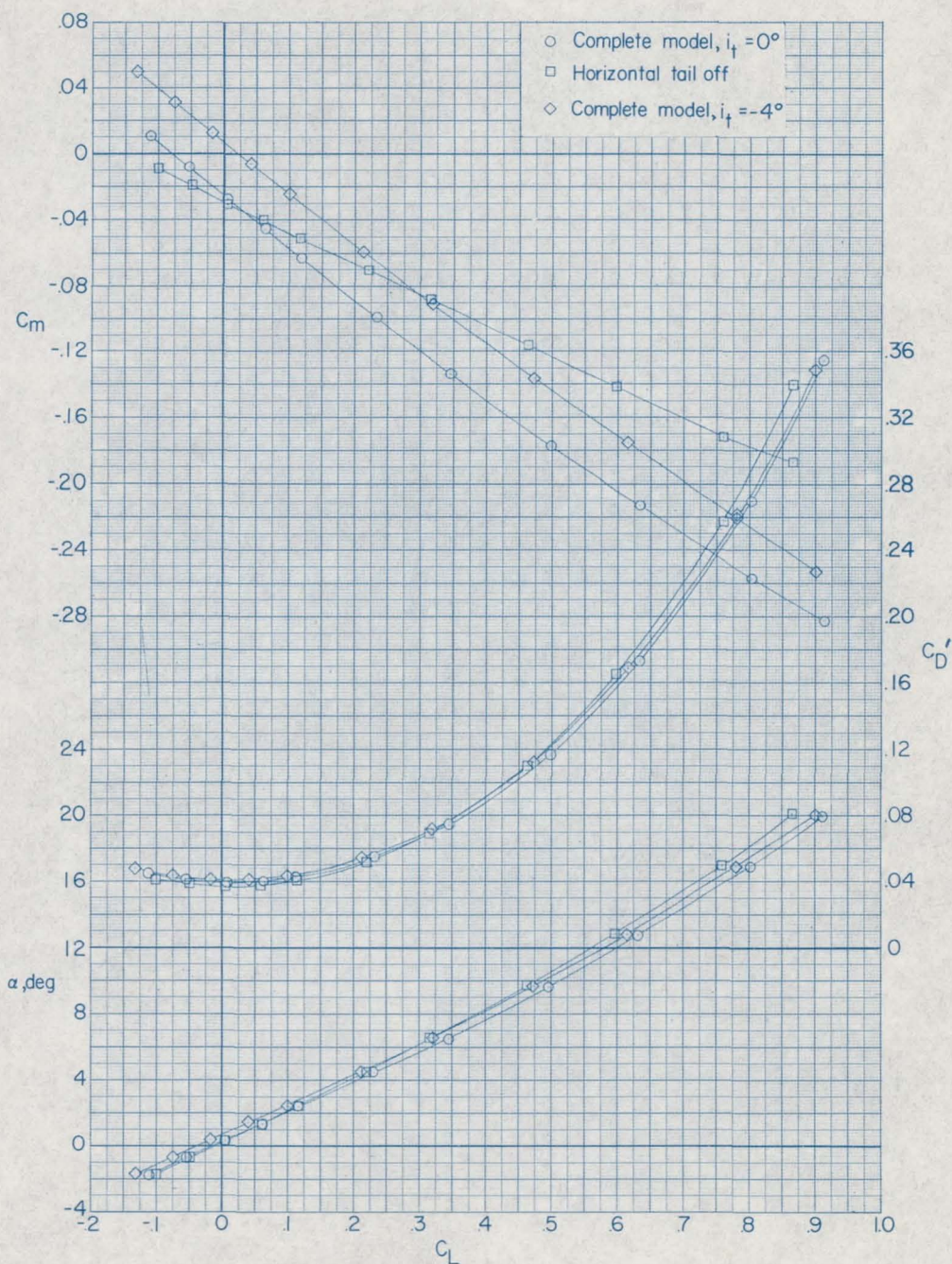
(a) M = 1.59.

Figure 7.- Effect of horizontal tail on aerodynamic characteristics in
pitch of 1/20-scale model of McDonnell F4H-1 airplane. β = 0°.

DECLASSIFIED
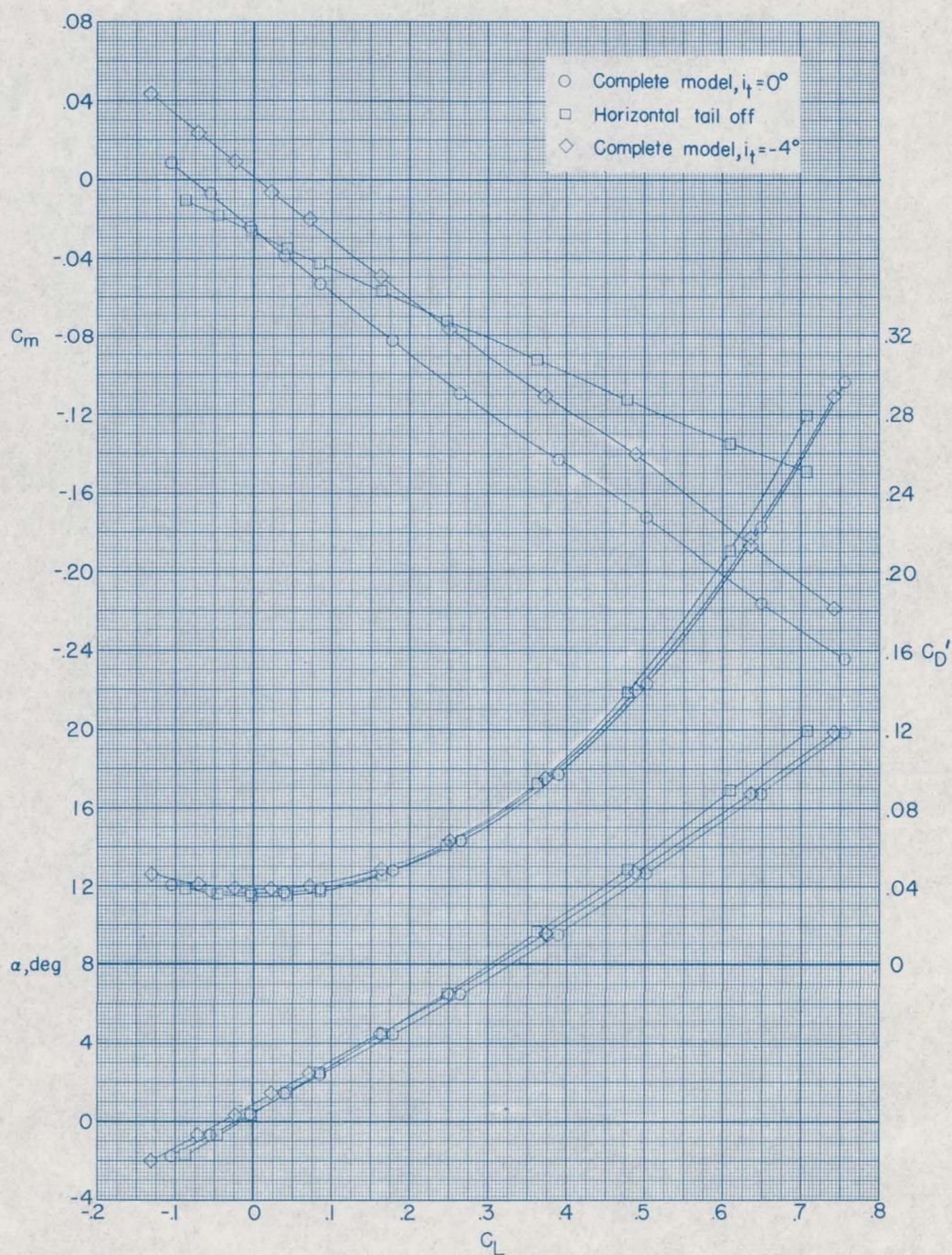
(b) M = 1.89.

Figure 7.- Continued.
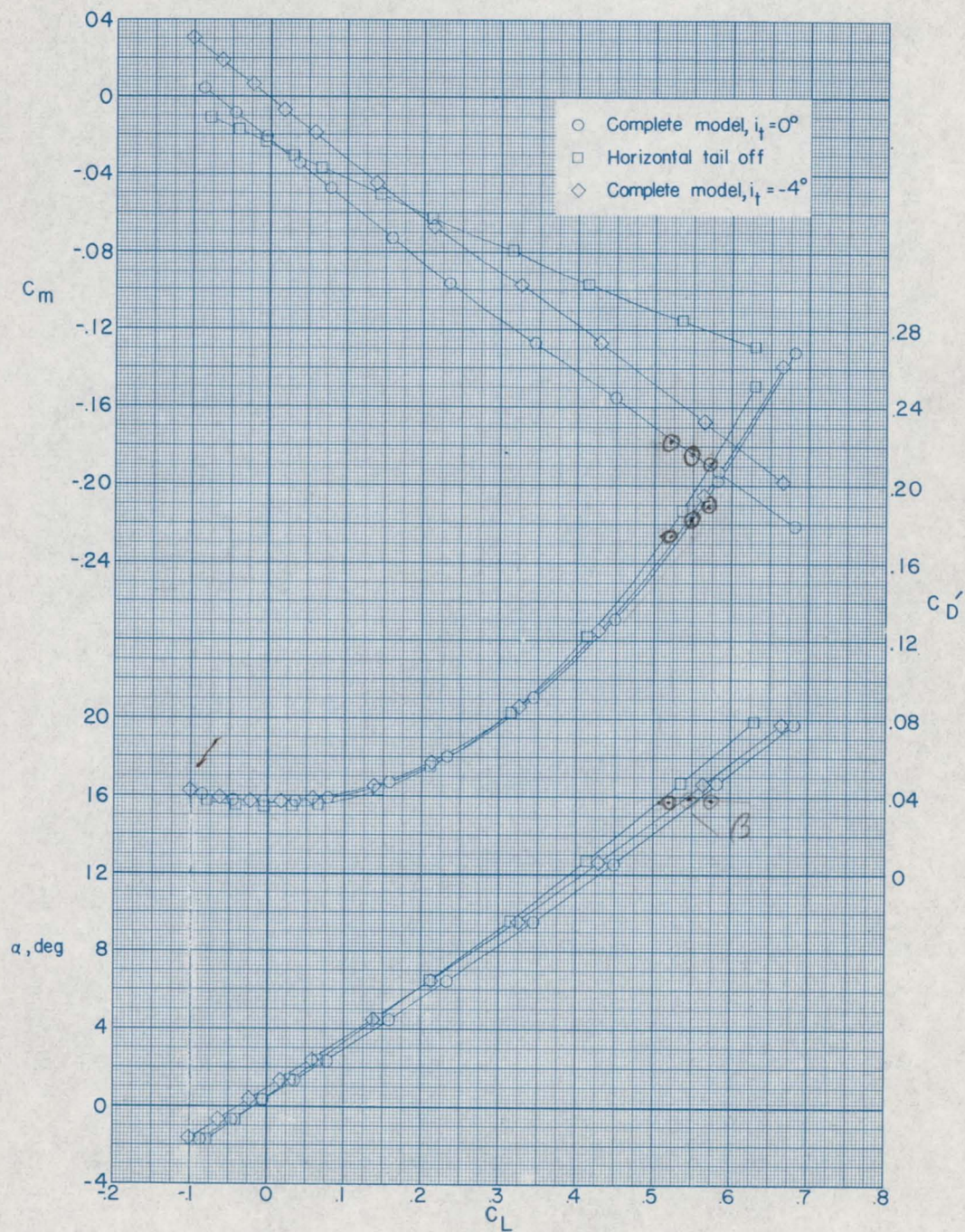
(c) M = 2.09.

Figure 7.- Concluded.
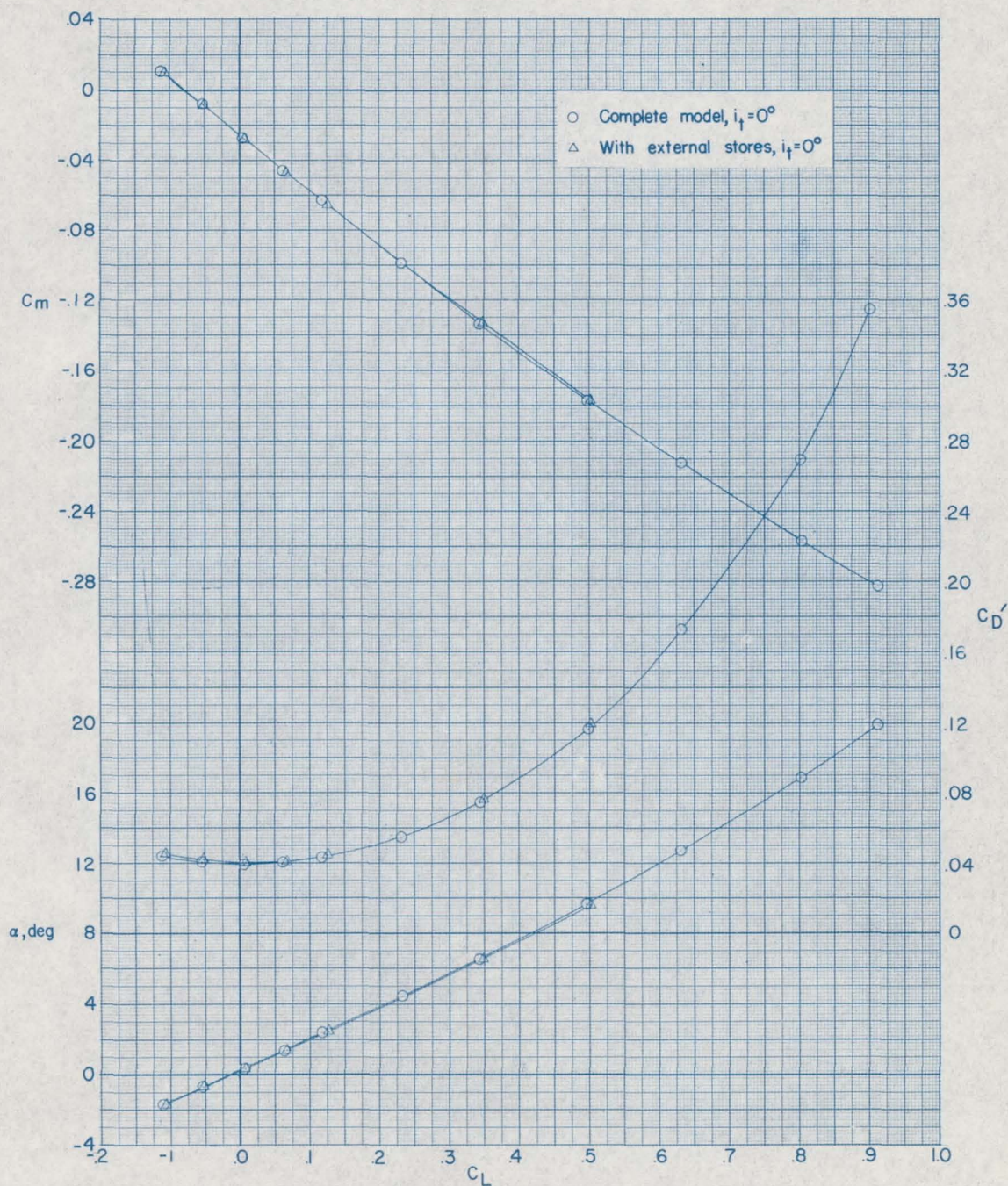
(a) M = 1.59.

Figure 8.- Effect of external stores on aerodynamic characteristics in pitch of 1/20-scale model of McDonnell F4H-1 airplane. $\beta = 0^\circ$.

DECLASSIFIED
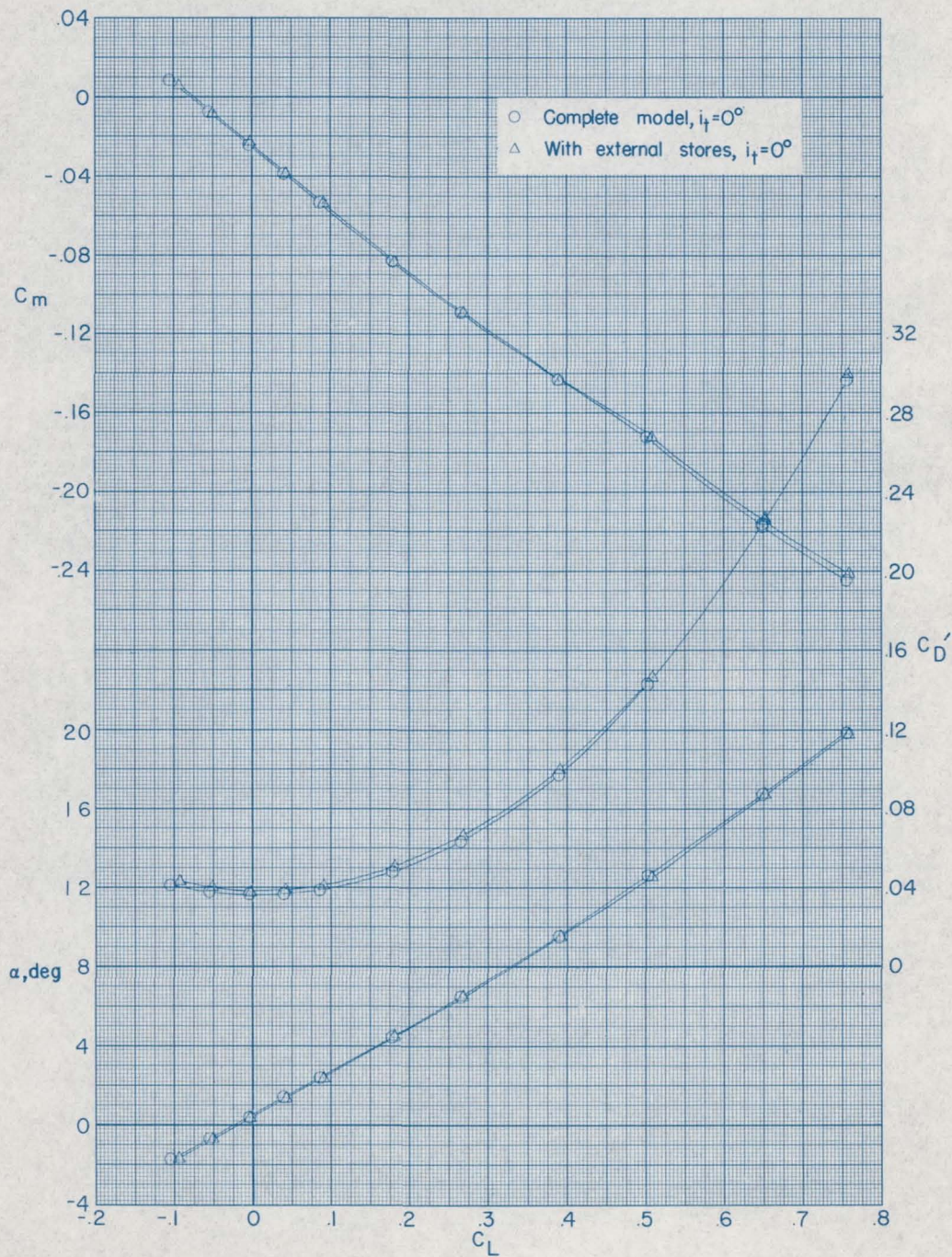
CONFIDENTIAL

(b) M = 1.89.

Figure 8.- Continued.

○   Complete model, $i_t = 0°$
△   With external stores, $i_t = 0°$
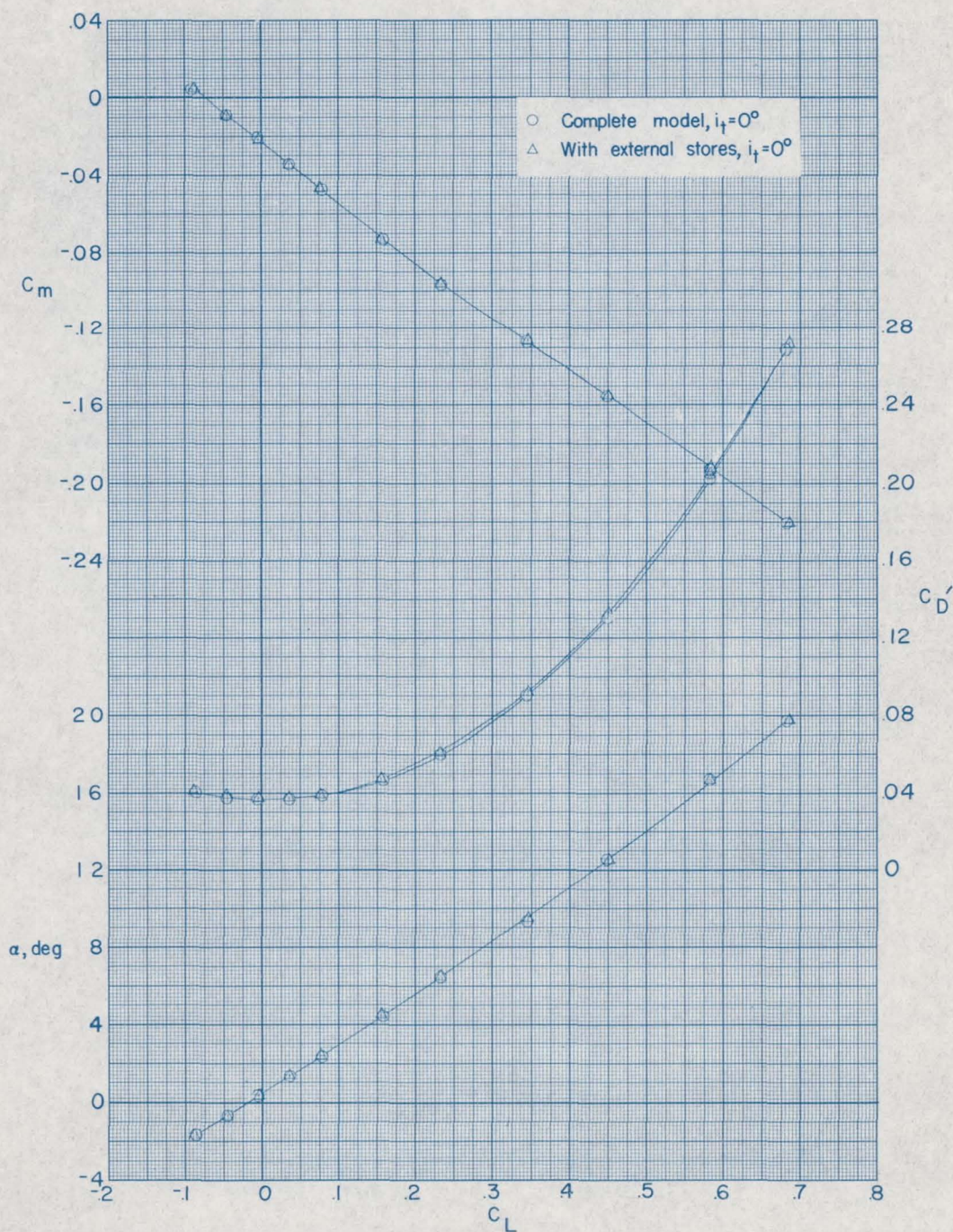
(c) M = 2.09.

Figure 8.- Concluded.

DECLASSIFIED
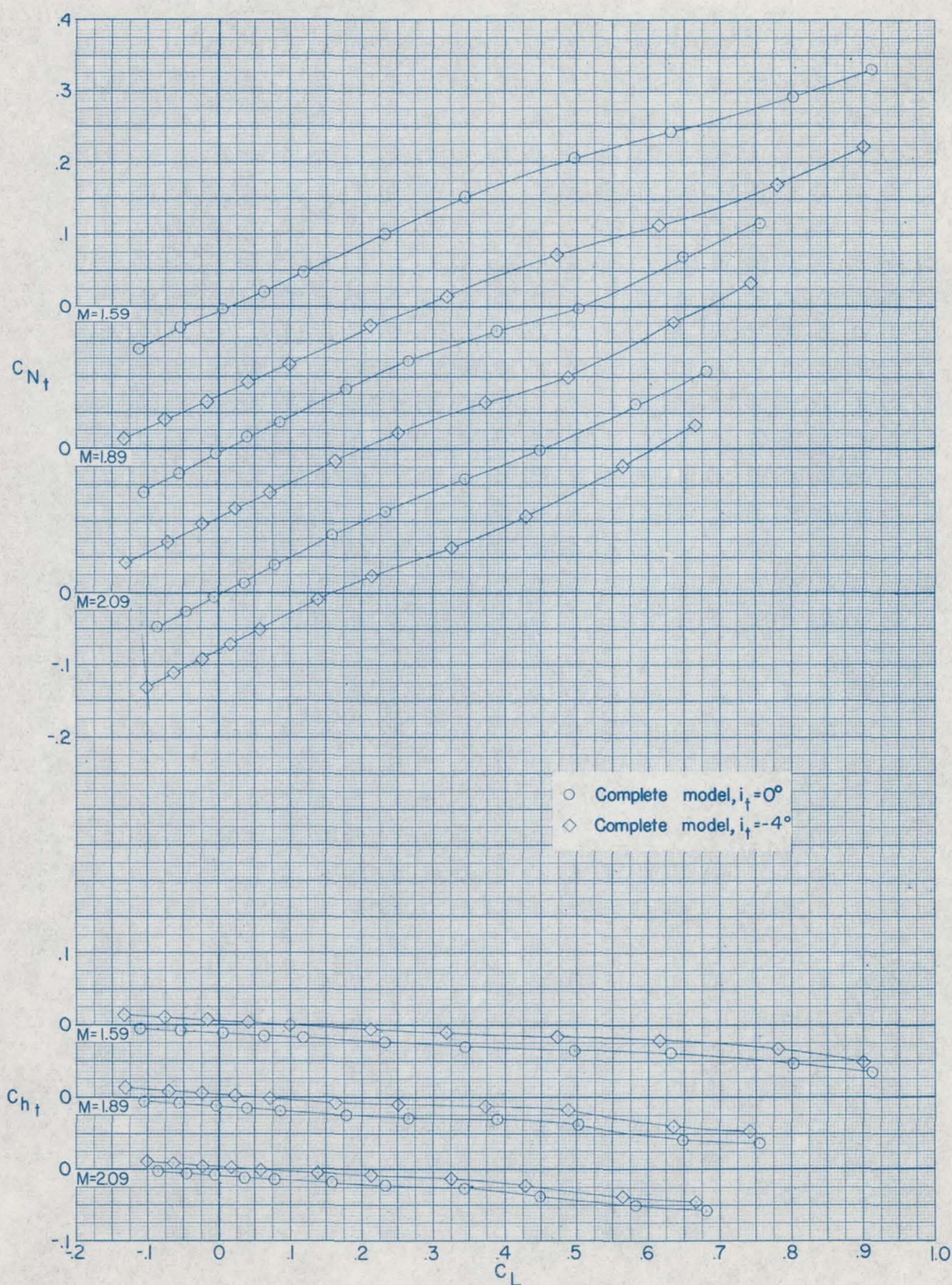
CONFIDENTIAL

Figure 9.- Effect of tail incidence on horizontal-tail hinge-moment coefficients and normal-force coefficients of 1/20-scale model of McDonnell F4H-1 airplane. $\beta = 0°$.

DE CLASSIFIED

CONFIDENTIAL

C_n

.04

.02

0

-.02

.02

.01

C_l

0

-.01

○ Complete model, $i_t = 0°$
△ Vertical tail off, $i_t = 0°$

.08

.04

0

-.04

C_Y

-.08

-.12

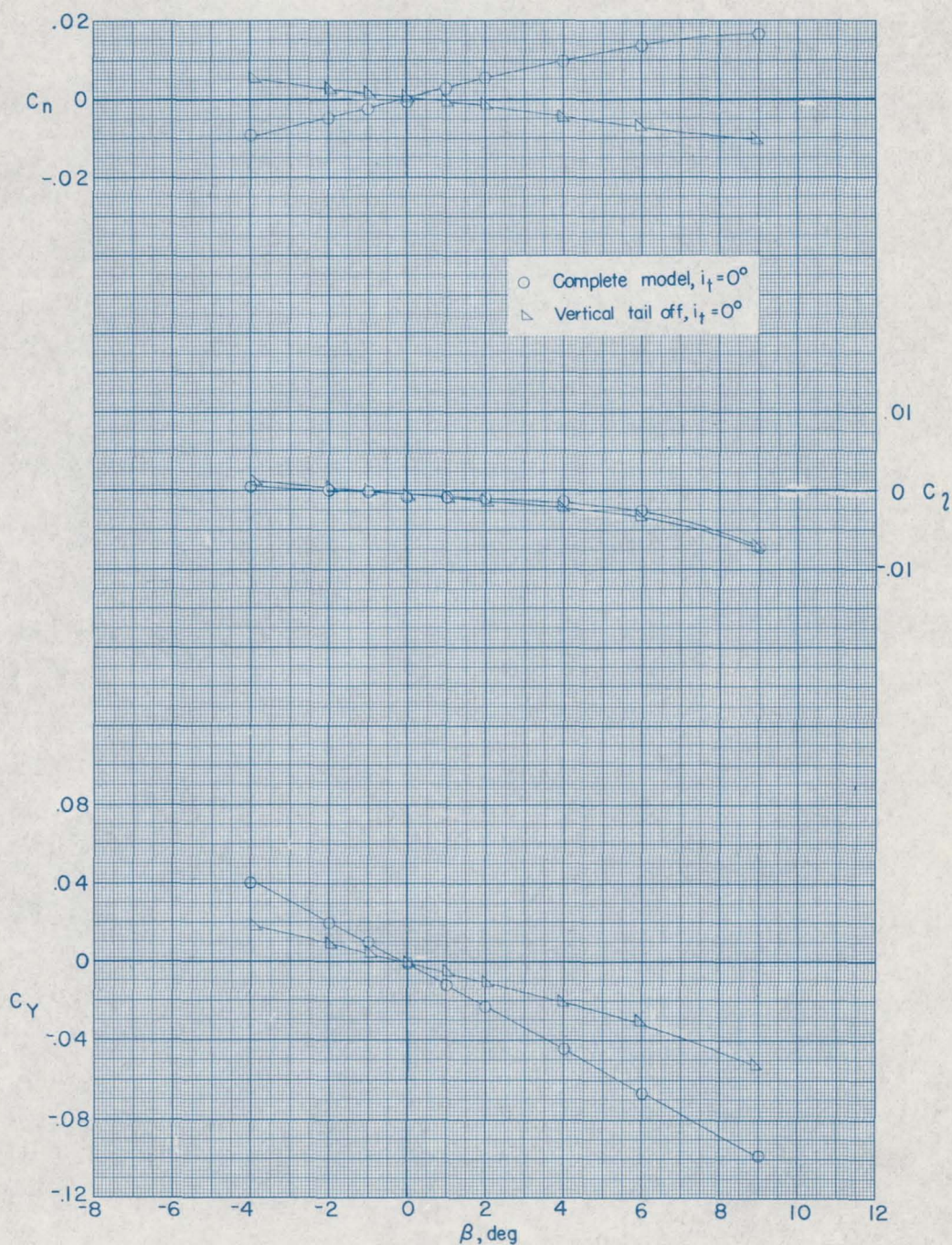-.16

-.20

-6   -4   -2   0   2   4   6   8   10   12   14

β, deg
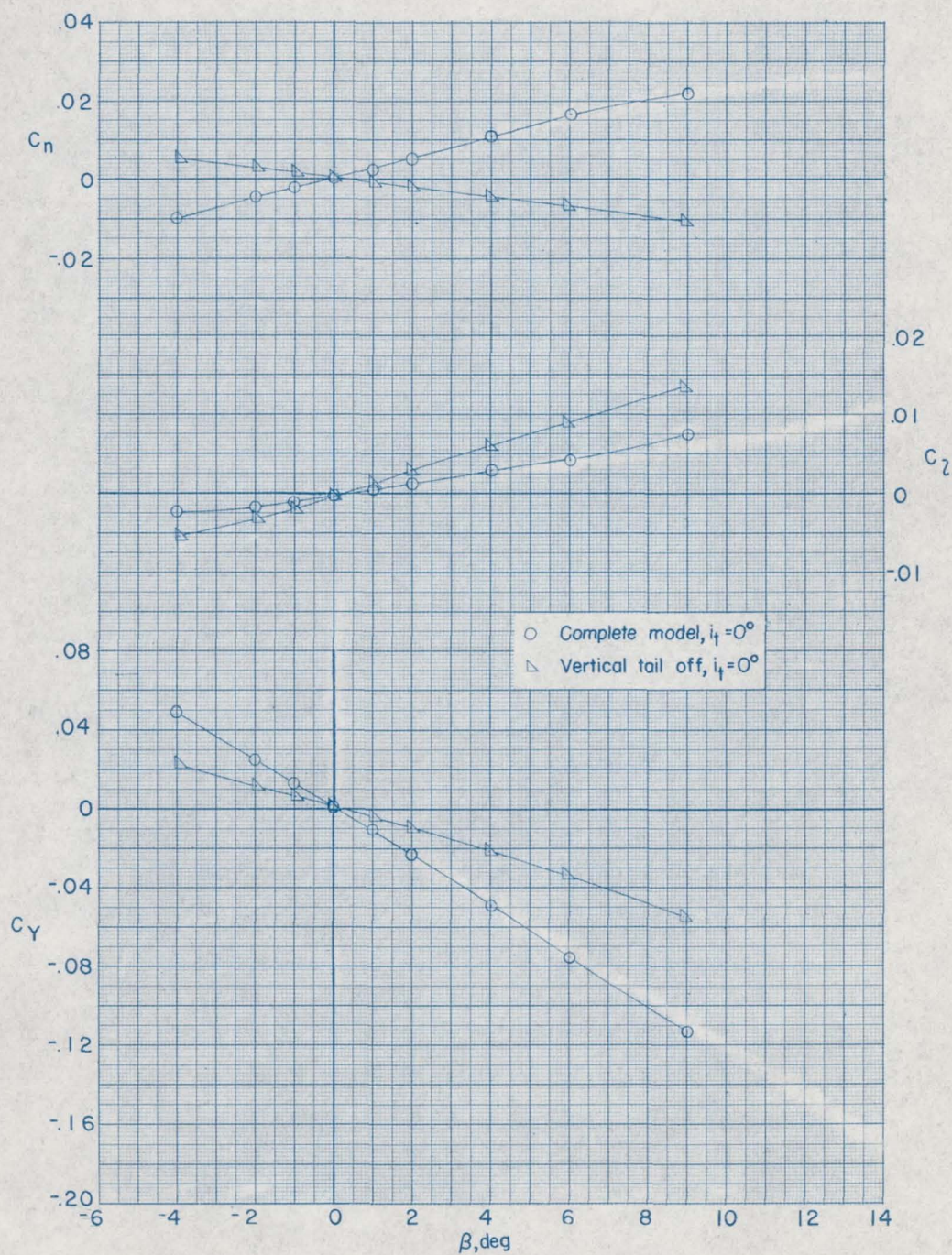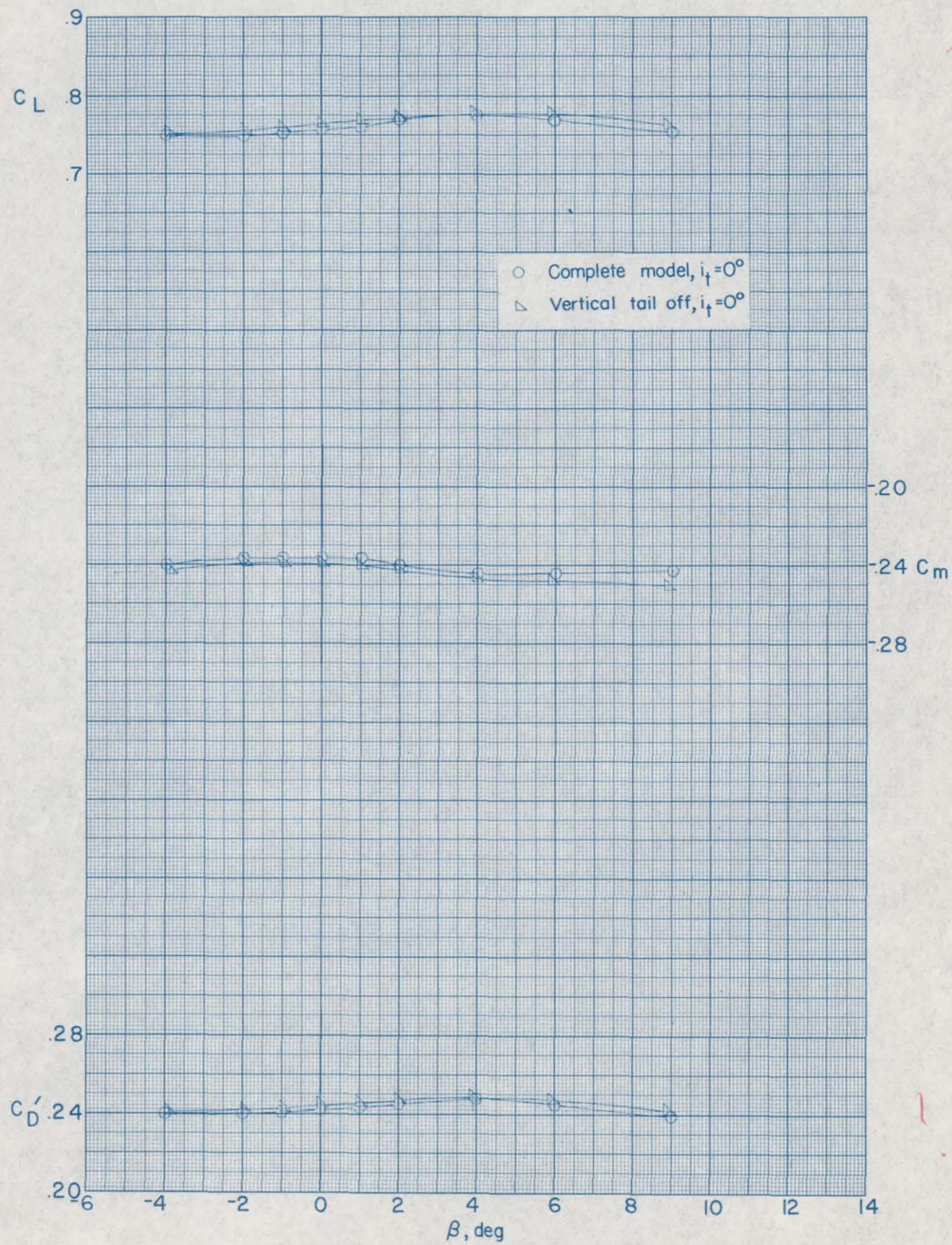
(a)   M = 1.59.

Figure 10.- Effect of sideslip on aerodynamic characteristics of
1/20-scale model of McDonnell F4H-1 airplane. $\alpha = 0.3°$.

CONFIDENTIAL

DECLASSIFIED

(a) Concluded.

Figure 10.- Continued.
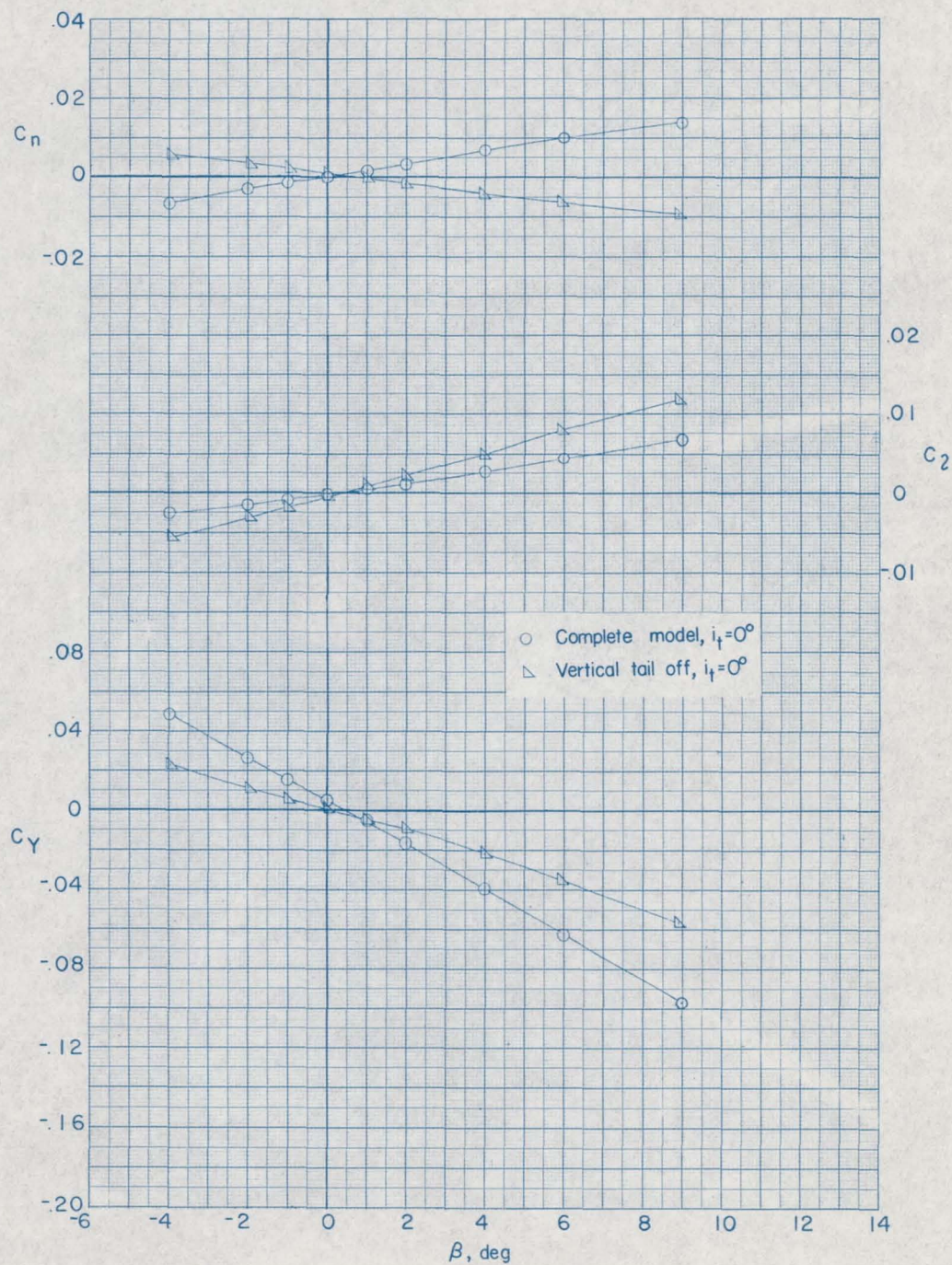
(b) M = 1.89.

Figure 10.- Continued.
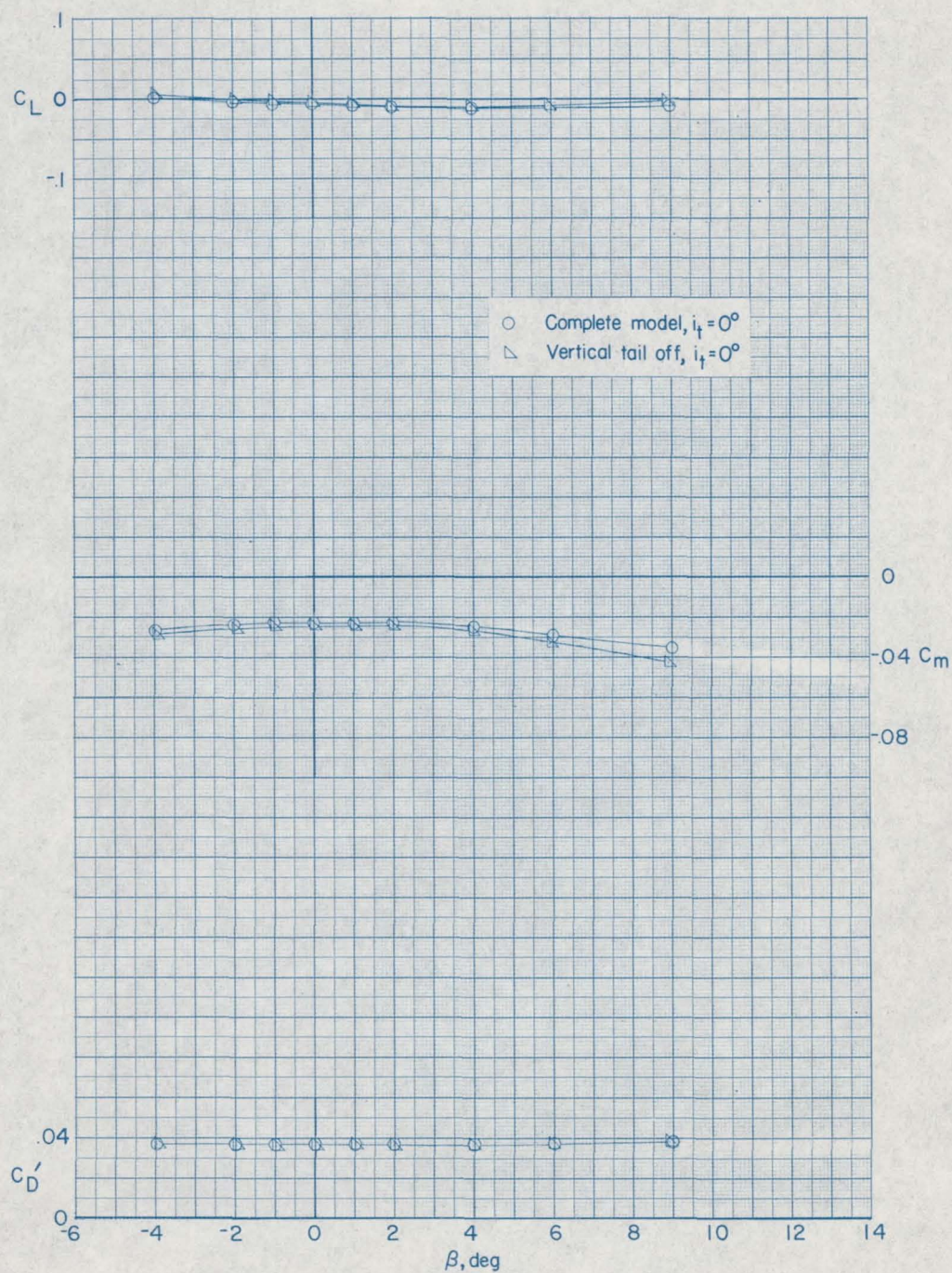
(b) Concluded.

Figure 10.- Continued.

DECLASSIFIED

○ Complete model, $i_t = 0°$
△ Vertical tail off, $i_t = 0°$

β, deg
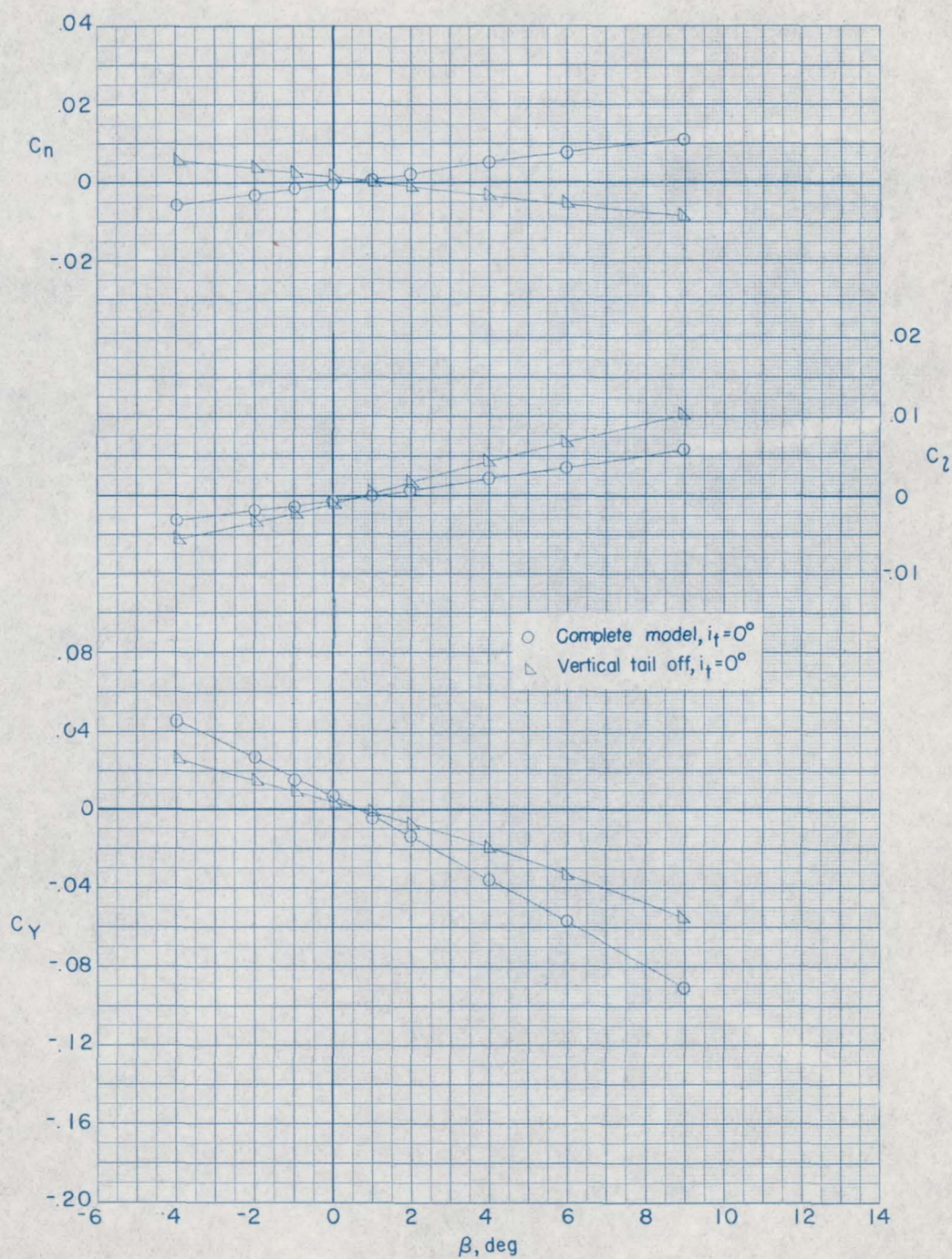
(c) M = 2.09.

Figure 10.- Continued.
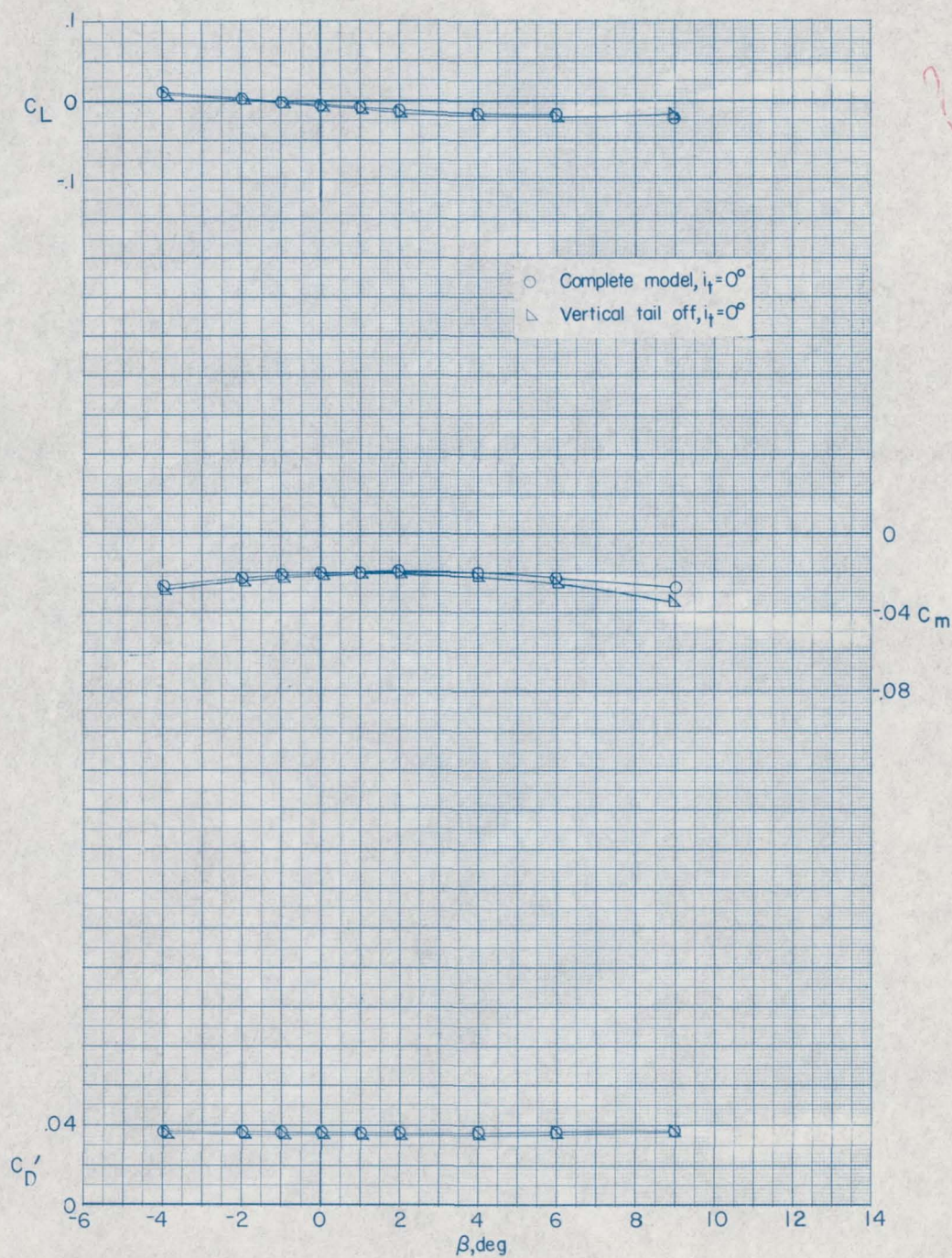
(c) Concluded.

Figure 10.- Concluded.
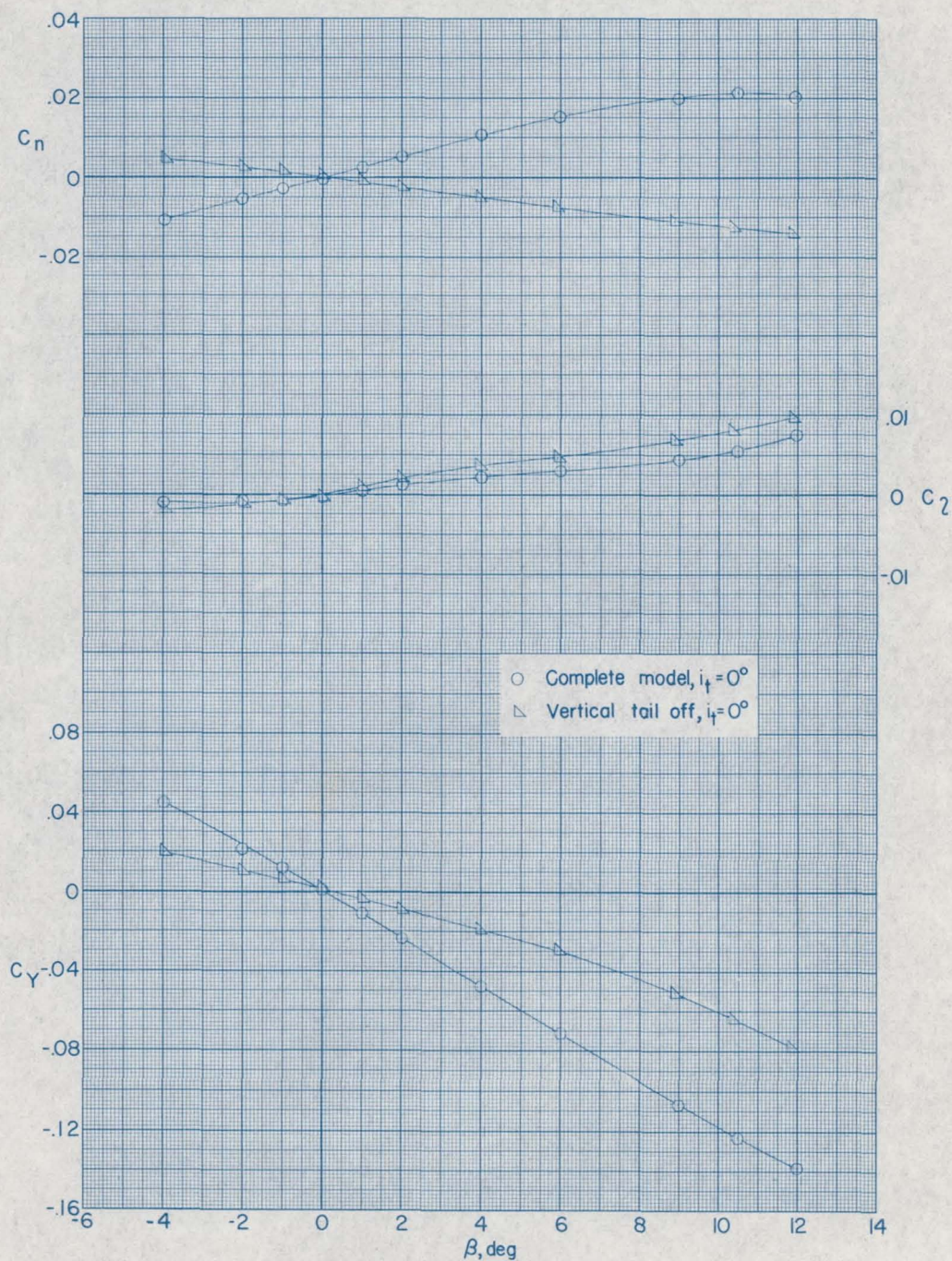
(a) M = 1.59.

Figure 11.- Effect of sideslip on aerodynamic characteristics of
1/20-scale model of McDonnell F4H-1 airplane. $\alpha = 8.5^{\circ}$.

(a) Concluded.

Figure 11.- Continued.
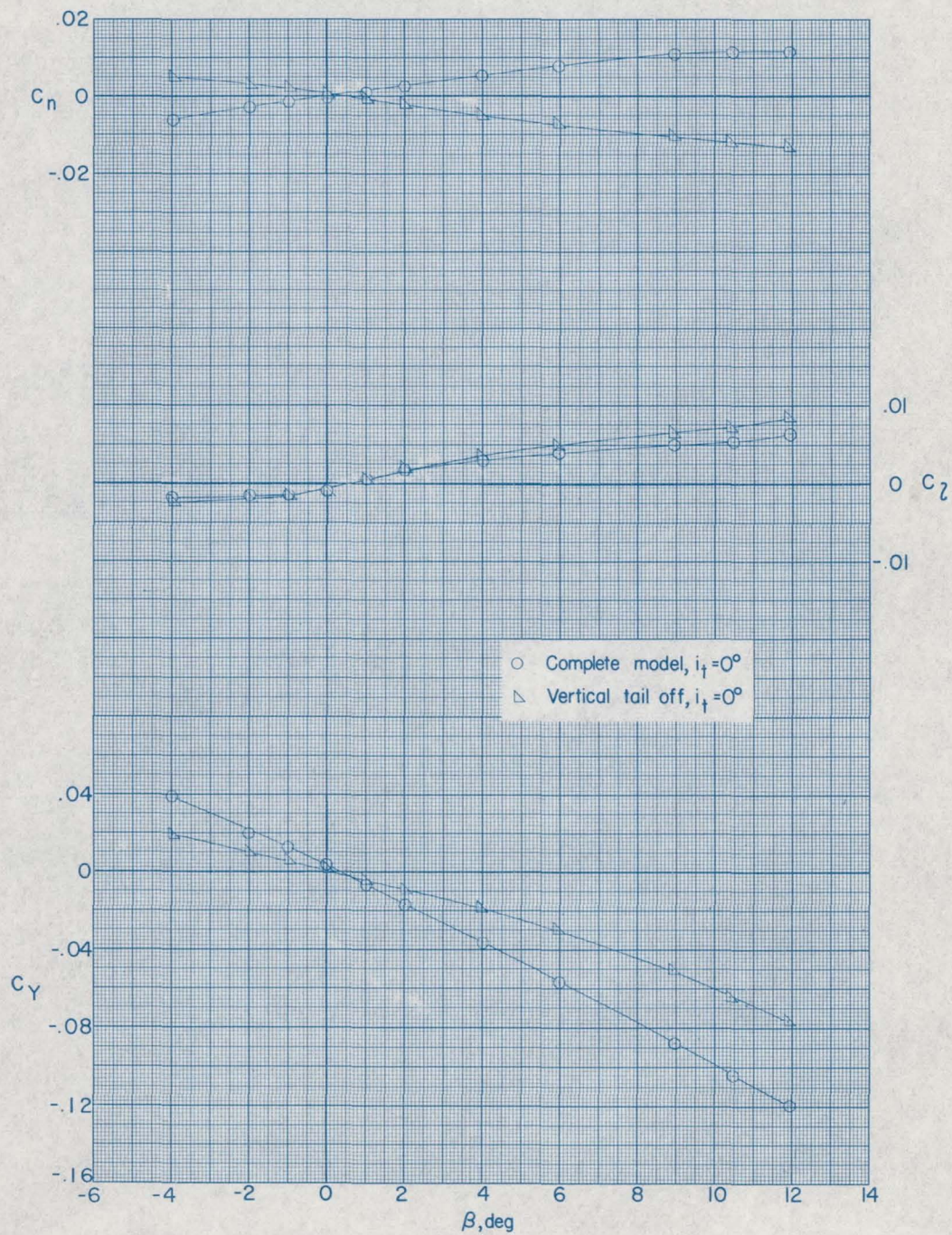
(b) M = 1.89.

Figure 11.- Continued.

DECLASSIFIED

(b) Concluded.

Figure 11.- Continued.

DECLASSIFIED

(c) M = 2.09.

Figure 11.- Continued.
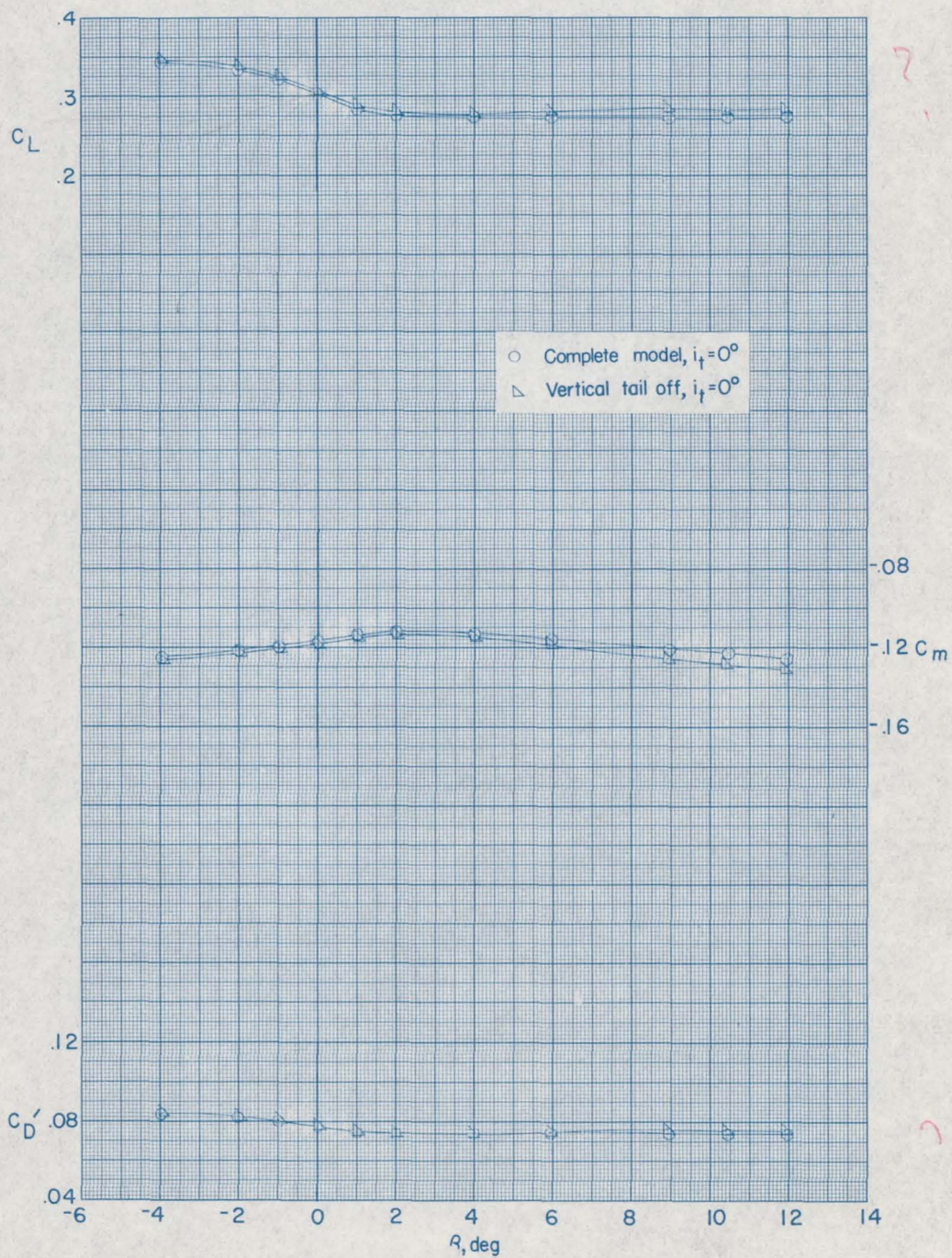
(c) Concluded.

Figure 11.- Concluded.

(a) M = 1.59.

Figure 12.- Effect of sideslip on aerodynamic characteristics of
1/20-scale model of McDonnell F4H-1 airplane. $\alpha = 15.7^\circ$.

DECLASSIFIED

(a) Concluded.

Figure 12.- Continued.

(b) M = 1.89.

Figure 12.- Continued.

(b) Concluded.

Figure 12.- Continued.
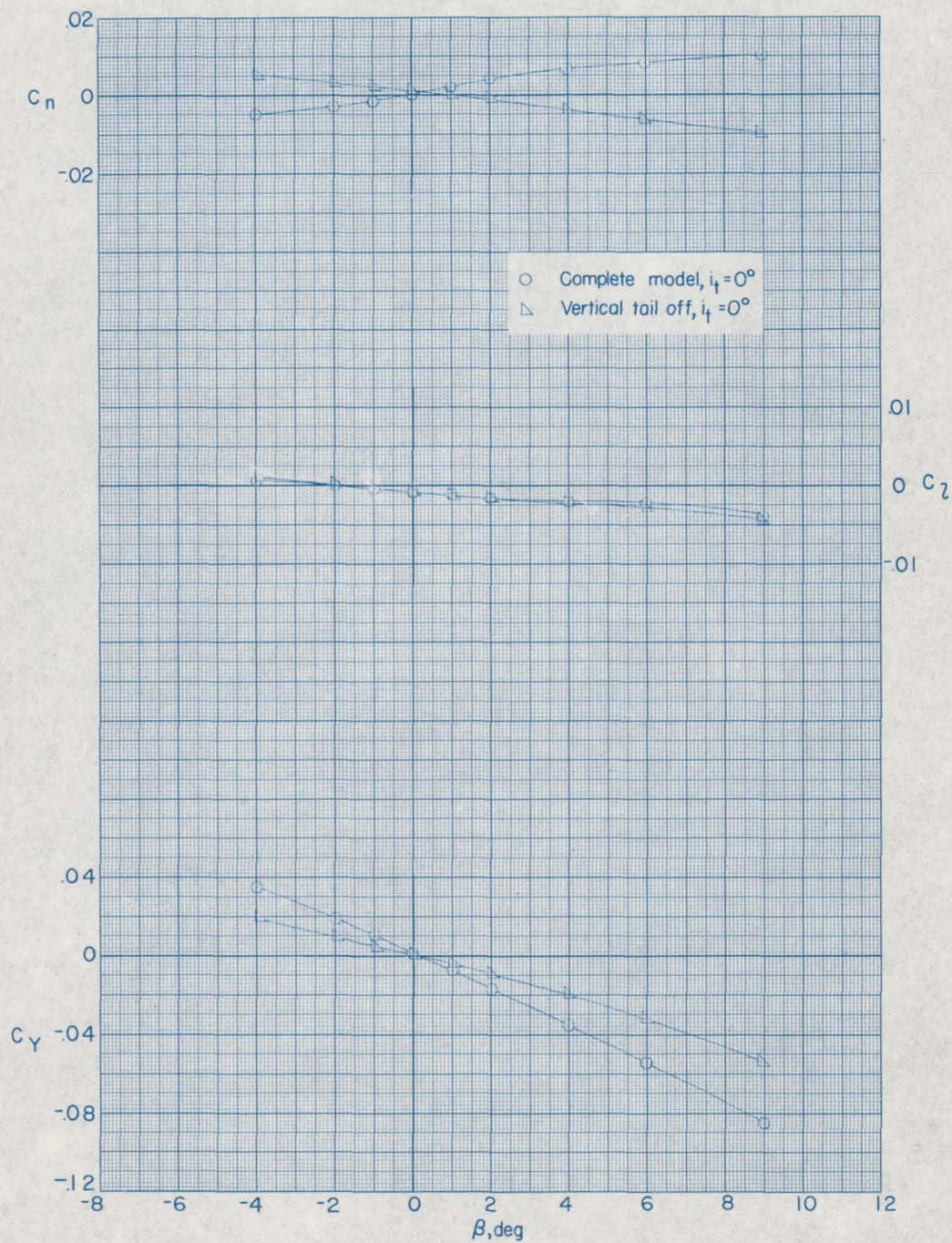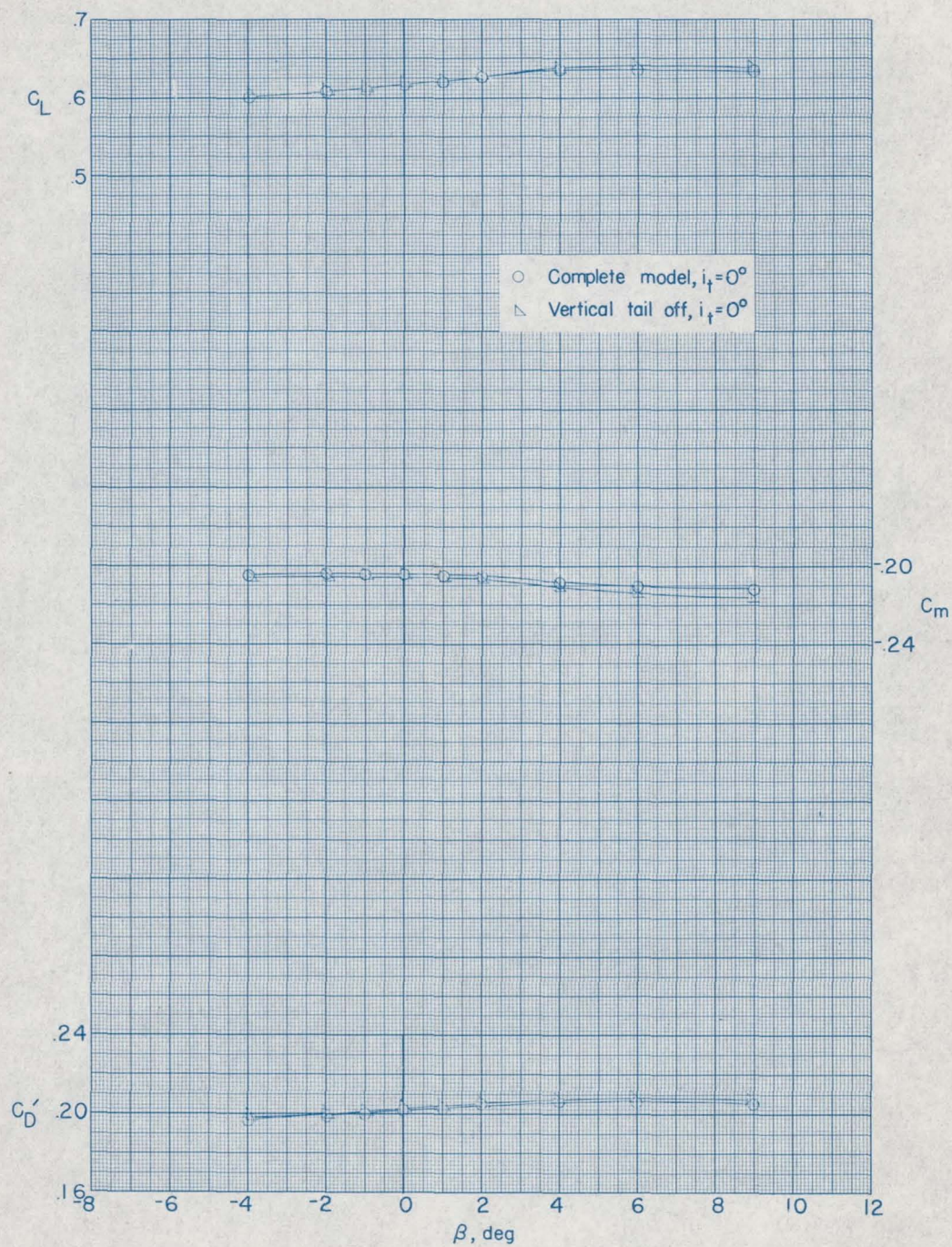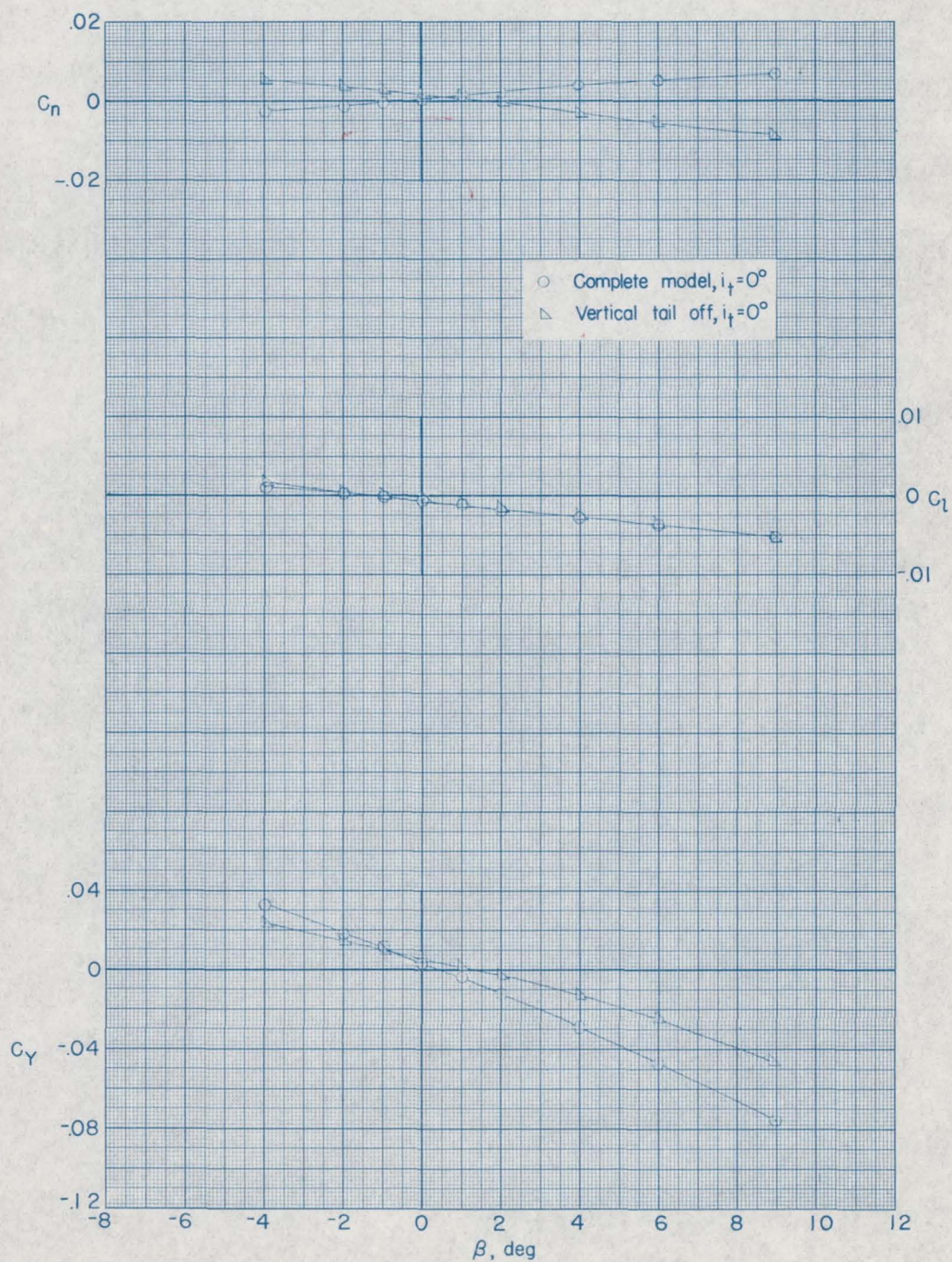
(c) M = 2.09.

Figure 12.- Continued.

DECLASSIFIED
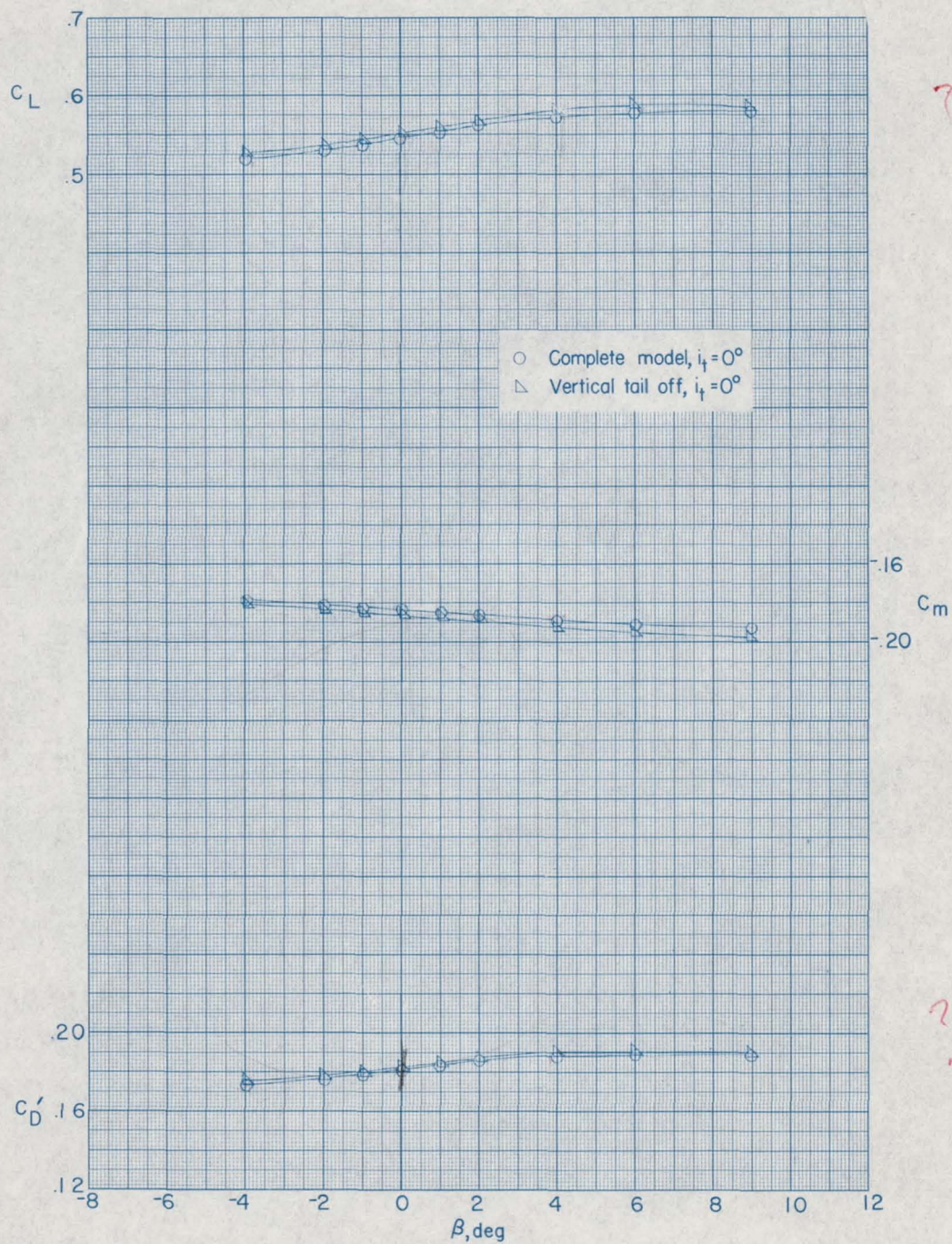
(c) Concluded.

Figure 12.- Concluded.

DECLASSIFIED

CONFIDENTIAL

INDEX

ABSTRACT

A limited investigation has been conducted in the Langley Unitary Plan wind tunnel at Mach numbers of 1.59, 1.89, and 2.09 to determine the aerodynamic characteristics in pitch and sideslip of a 1/20-scale model of the McDonnell F4H-1 airplane. The model had a wing with 45° sweepback at the quarter-chord line, aspect ratio of 2.821, and taper ratio of 0.167. A configuration consisting of the model with four semi-submerged fuselage stores was also investigated. This is a data report for limited distribution and does not contain any analysis.